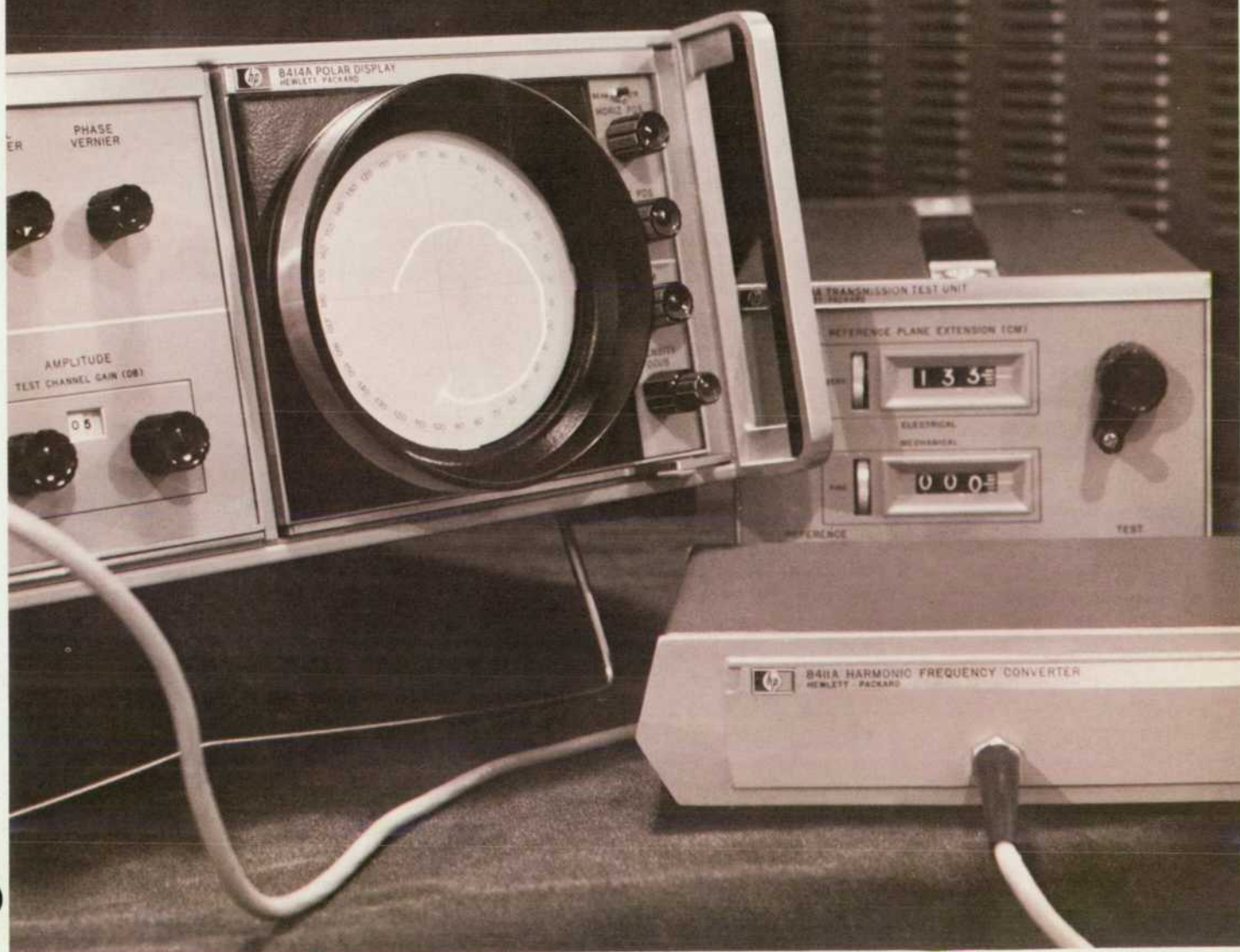


# HEWLETT-PACKARD JOURNAL

**Cover: A NEW MICROWAVE INSTRUMENT SWEEP-  
MEASURES GAIN, PHASE, IMPEDANCE  
WITH SCOPE OR METER READOUT; page 2**

**See Also: THE MICROWAVE ANALYZER IN THE  
FUTURE; page 11  
S-PARAMETERS THEORY AND  
APPLICATIONS; page 13**



**FEBRUARY 1967**

© Copr. 1949-1998 Hewlett-Packard Co.



Fig. 1. Automatic Network Analyzer for measuring complex impedances, gain, loss, and phase shift from 0.11 to 12.4 GHz consists of (l. to r.), Model 8411A Harmonic Frequency Converter, Model 8410A Main Frame, and a plug-in display module (either Model 8413A Phase-Gain Indicator or Model 8414A Polar Display). Network Analyzer makes swept or single-frequency measurements. See Fig. 8 for other system components.

## An Advanced New Network Analyzer for Sweep-Measuring Amplitude and Phase from 0.1 to 12.4 GHz

*The information obtainable with a new network analyzer greatly improves microwave design practices, especially where phase information is important.*

A NEW MICROWAVE NETWORK ANALYZER developed in the *-hp-* microwave laboratory promises to be of major importance in many electronic fields, especially those concerned with the phase properties of microwave systems and components. The new instrument sweep-measures the magnitude and phase of reflection and transmission coefficients over the range from 110 MHz to 12.4 GHz. This makes it possible for the analyzer to completely characterize active and passive devices, since nearly every parameter of interest for high-frequency devices can be measured including gain, attenuation, phase, impedance, admittance and others.

The new analyzer represents a major step in the continuing trend to automation in microwave measurements, a trend recognized in several articles in this publication and elsewhere\*. Systems that are especially aided by the kinds of automated measurements the analyzer makes are the modern systems that emphasize phase properties, such as electronically-scanned radar and monopulse and doppler radar. Similarly, optimum use of the new high-frequency solid-state devices that make systems such as phased-array radars economically practical is dependent on sophisticated measurements. The reason for this de-

\* See references on page 9.

### **-hp- Journal readers:**

*We believe you who work with frequencies above 100 MHz will be especially interested in this issue because it discusses an important new system that measures gain, phase, impedance, admittance and attenuation on a swept basis from 110 MHz to 12.4 GHz. In other words the system will measure all network parameters not only of passive networks and devices but also of transistors and even of negative real impedances. Readout is on a meter or on a scope which presents measured performance over a whole frequency band at a glance.*

*The new system leads to wider use of the familiar quantities we usually call reflection and transmission coefficients. These coefficients are also known as 'scattering parameters', and using them in combination with the new system leads to more sophisticated design techniques including computerized design. An informative article about scattering parameters begins on p. 13.*

*Obviously, the new system is a powerful tool for the engineer. In addition, it has important implications for the whole microwave engineering field in the future. This is also discussed in this issue (p. 11) by Paul Ely, engineering manager of our microwave laboratory.*

*I invite your attention to what we believe is unusually important microwave information.*

Sincerely, Editor

pendence is that these solid-state devices can best be utilized in new functions if they can be completely characterized and understood.

The analyzer characterizes networks by measuring their complex small-signal parameters. The particular types of parameters measured are called the scattering or "s" parameters. These parameters have proved a valuable tool for the design engineer because of their inherent ease of measurement, their design advantages and the intuitive insight they provide. A separate article in this issue deals with their theory and describes new design practices developed with them at Hewlett-Packard.

### Network Analyzer Concept

The concept of the network analyzer follows naturally from network-parameter theory. Measuring s-parameters is a matter of measuring (a) the ratio of the magnitudes and (b) the relative phase angles of response and excitation signals at the ports of a network with the other ports terminated in a specified 'characteristic' or reference impedance. It is not difficult to define the basic elements of a network analyzer system to perform these measurements (Fig. 3). First, a source of excitation is required. Then a transducer instrument is needed to convert the excitation signal and the response signals produced by the unknown to a set of output signals containing the network information (a dual-directional coupler for measuring the complex reflection coefficient  $s_{11}$  is illustrated). Next, an instrument capable of measuring magnitude ratio and phase difference is used to extract the pertinent information from the test signals. A readout mechanism to present the data completes the basic network analyzer.

The above is the concept that has been followed in designing the new network analyzer. A further refinement of the concept is the use of a plug-in readout. Although the network parameter data are the same for each application (i.e., magnitude and phase), the form in which the data are most useful depends upon the application.

**Table I System Components**

MODEL	FUNCTION	RANGE
8410A Network Analyzer Main Frame	Mainframe for readout modules, includes tuning circuits, IF amplifiers, and precision IF attenuator.	0.11 to 12.4 GHz when used with Model 8411A.
8411A Harmonic Frequency Converter	Converts 2 RF input signals 0.11 to 12.4 GHz into 20-MHz IF signals.	0.11 to 12.4 GHz when used with the 8410A. Impedance 50 ohms.
8413A Phase-Gain Indicator	Plug-in module for 8410A Mainframe provides meter display of relative amplitude and phase between input signals, auxiliary outputs for scope or X-Y recorder.	Full scale $\pm 3, 10, 30$ dB and $\pm 6, 18, 60, 180$ degrees. Auxiliary outputs 50 mV/dB and 10 mV/degree.
8414A Polar Display Unit	Plug-in module for 8410A Mainframe. CRT polar display of amplitude and phase. X-Y outputs for high resolution polar and Smith Chart impedance plots.	Internal graticule CRT for nonparallax viewing. Amplitude calibration in five linear steps. Phase in $10^\circ$ intervals through $360^\circ$ . Smith Chart overlays for direct impedance readout (normalized to 50 ohms).
8740A Transmission Test Unit	Simplifies RF input and test device connection for attenuation or gain test. Accepts RF input signal from source and splits into reference and test channels for connection to 8411A and the unknown device. Calibrated line stretcher balances out linear phase shift when test device is inserted.	0.11 to 12.4 GHz, Impedance 50 ohms.
8741A Reflection Test Unit	Wide-band reflectometer, phase balanced for swept or spot frequency impedance tests below 2 GHz. Accepts RF input and provides connections for unknown test device and 8411A. Movable reference plane.	0.11 to 2.0 GHz.
8742A Reflection Test Unit	Ultra-wide band reflectometer, phase balanced for impedance tests above 2.0 GHz. Movable reference plane.	2.0 to 12.4 GHz



Fig. 2. Typical test setup using new Network Analyzer (top center) to sweep-measure transmission of microwave filter. Magnitude and phase are measured on Analyzer meter and presented as a function of frequency on oscilloscope. Magnitude and phase can also be presented in polar form on a Polar Display scope which plugs in, in place of Phase Gain Indicator and will feed external recorder.

Other pieces of auxiliary equipment will, in general, be added to complete a specific measurement. Examples would be bias supplies for active devices and matched loads for termination purposes.

Here then is a very flexible system that defines completely the complex parameters of an active or passive network. It provides this information, much of which was previously very difficult or prohibitively expensive to obtain, over a huge frequency range with an ease and rapidity that consistently intrigues those who see it the first time. Specific features of the network analyzer are the following:

1. One system measures both magnitude and phase of all network parameters from 110 MHz to 12.4 GHz. The measurements can be made at a single frequency or on a swept frequency basis over octave bandwidths.
2. The analyzer combines wide dynamic range with high measurement resolution. Direct dynamic display range is 60 dB in magnitude and  $360^\circ$  of phase. Precise internal attenuators and a calibrated phase offset allow expanded measurements with better than 0.1 dB resolution in magnitude and  $0.1^\circ$  in phase.
3. It is accurate. Precision components are used throughout to assure basic accuracy. The two-channel comparative technique removes error terms caused by the source and variations common to both channels.
4. A choice of display allows the data to be presented in the most useful form for the specific measurement. The measured data are also provided in analog form for external oscilloscope, recorder, or digital display.

### Frequency Translation by Sampling

Figs. 1 and 8 show the elements of the analyzer system and Table I lists the elements, their functions, and their frequency ranges. The basic analyzer (Fig. 1) consists of three units: a main frame, either of two plug-in display modules, and a harmonic frequency converter. The transducer instruments for reflection and transmission (Fig. 8) complete the system.

The key technique that allows the new microwave network analyzer to measure complex ratio is the technique of frequency translation by sampling. The block diagram of the basic analyzer shown in Fig. 4 is helpful to understand this technique. Sampling as used in this system is a special case of heterodyning, which translates the input signals to a lower, fixed IF frequency where normal circuitry can be used to measure amplitude and phase relationships. The principle is to exchange the local oscillator of a conventional heterodyne system with a pulse generator which generates a train of very narrow pulses. If each pulse within the train is narrow compared to a period of the applied RF signal, the sampler becomes a harmonic mixer with equal efficiency for each harmonic. Thus sampling-type mixing has the advantage that a single system can operate over an extremely wide input frequency range. In the case of the network analyzer this range is 110 MHz to 12.4 GHz.

In order to make the system capable of swept frequency operation, an internal phase-lock loop keeps one channel of the two-channel network analyzer tuned to the incoming signal. Tuning of the phase-lock loop is entirely automatic. When the loop is unlocked, it automatically tunes back and forth across a portion of whatever octave-wide frequency band has been selected by the user. When any harmonic of the tracking-oscillator frequency falls 20 MHz below the input frequency, i.e., when  $f_{in} - nf_{osc} = 20$  MHz, the loop stops searching and locks. Search and lock-on are normally completed in

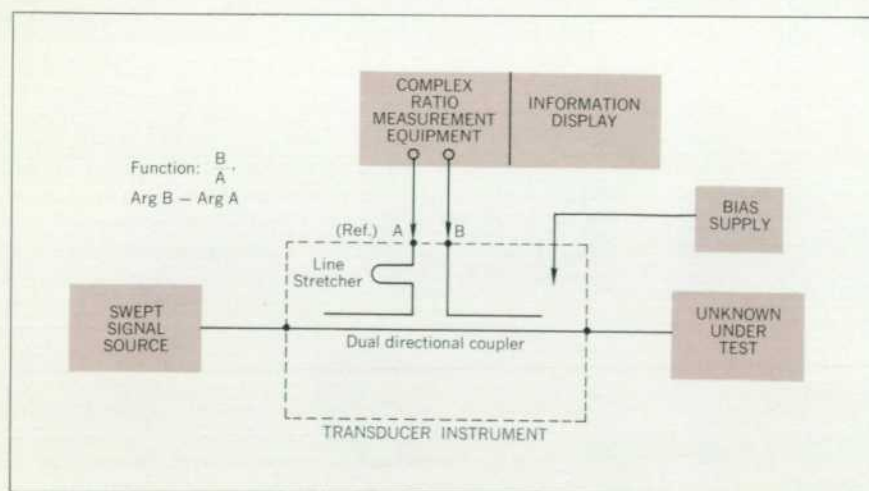
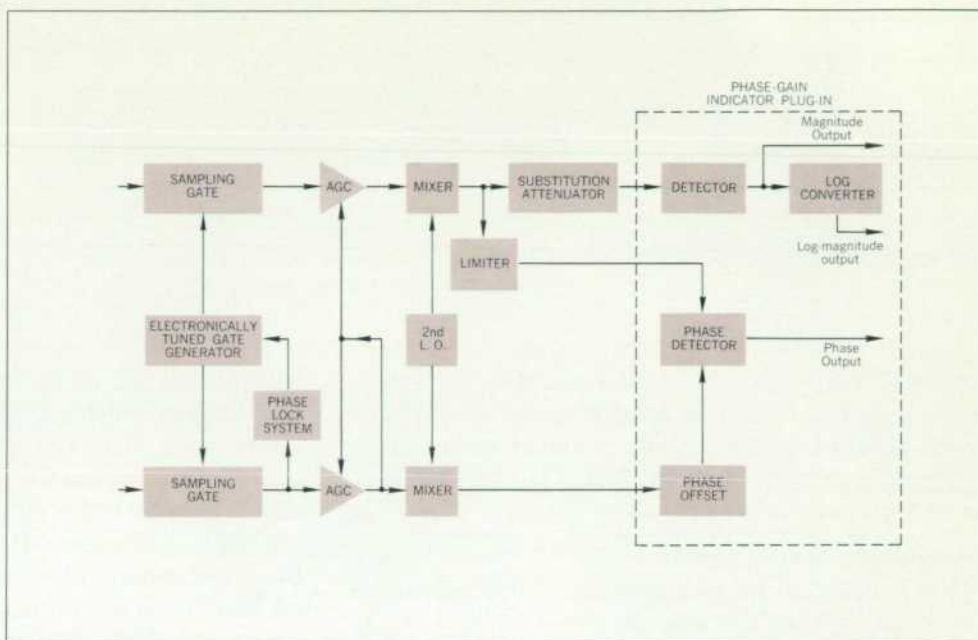


Fig. 3. Network Analyzer concept follows from network theory, as explained in text.

Fig. 4. Basic system used in Analyzer to achieve frequency translation by a sampling technique.



about 20  $\mu$ s. The loop will remain locked for sweep rates as high as 220 GHz/sec (a rate corresponding to about 30 sweeps per second over the highest frequency band, 8 to 12.4 GHz).

The IF signals reconstructed from the sampler outputs are both 20-MHz signals, but since frequency conversion is a linear process, these signals have the same relative amplitudes and phases as the microwave reference and test signals. Thus gain and phase information are preserved, and all signal processing and measurements take place at a constant frequency.

Referring again to Fig. 4, the IF signals are first applied to a pair of matched AGC (automatic gain control) amplifiers. The AGC amplifiers perform two functions: they keep the signal level in the reference channel constant, and they vary the gain in the test channel so that the test signal level does not change when variations common to both channels occur. This action is equivalent to taking a ratio and removes the effects of power variations in the signal source, of frequency response characteristics common to both channels, and of similar common-mode variations.

Before the signals are sent to the display unit, a second frequency conversion from 20 MHz to 278 kHz is performed. To obtain the desired dB and degree quantities, the phase-gain indicator plug-in display unit (Fig. 4) contains a linear phase detector and an analog logarithmic converter which is accurate over a 60 dB range of test signal amplitudes. Ratio (in dB) and relative phase can be read on the meter of the display unit if desired, but the plug-in also provides calibrated dc-coupled voltages proportional to gain (as a linear ratio or in dB) and phase

for display on the vertical channels of an oscilloscope or X-Y recorder. If the horizontal input to the oscilloscope or recorder is a voltage proportional to frequency, the complete amplitude and phase response of the test device can be displayed.

#### Polar Display Unit

The Polar Display Unit (Fig. 5) converts polar quantities of magnitude and phase into a form suitable for display on a CRT. This is accomplished by using two balanced-modulator phase detectors. The phase of the test channel is shifted 90° with respect to the reference channel before being applied to the balanced modulator. The output of one modulator is proportional to  $A \sin \theta$ . This signal is amplified and fed to the vertical plates of

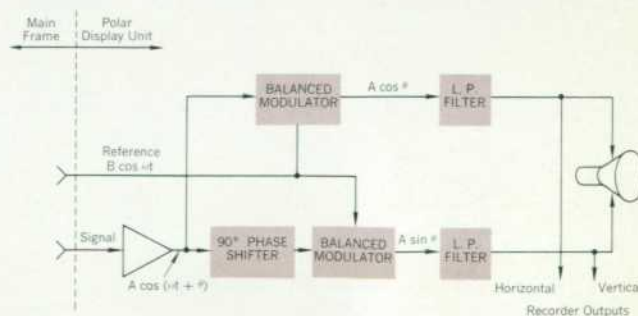


Fig. 5. Block diagram of basic Polar Display Unit which converts polar magnitude and phase information to be presented on its self-contained CRT.

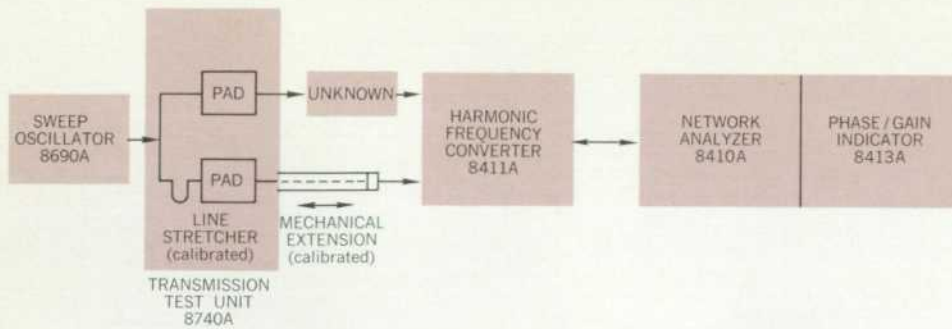


Fig. 6. Block diagram of transmission test with new Network Analyzer.  $S$ -parameters  $s_{12}$  and  $s_{21}$  can be measured thus.

the CRT. The output of the other modulator is proportional to  $A \cos \theta$  and this signal is applied to the horizontal plates of the CRT. Thus, the polar vector can be displayed in rectangular coordinates of an oscilloscope or an X-Y recorder.

### Transmission Measurements

Fig. 6 illustrates the measurement of the transmission coefficients  $s_{21}$  and  $s_{12}$  with the network analyzer. As explained on p. 13, these parameters are the forward and reverse transmission gain of the network when the output and input ports, respectively, are terminated in the reference or characteristic impedances. Transmission measurements are used to determine bandwidth, gain, insertion loss, resonances, group delay, phase shift and distortion, etc. For these measurements a swept-frequency source provides an input to the transmission test unit, which consists of a power divider, a line stretcher and two fixed attenuators. The transmission test unit has two outputs, a reference channel and a test channel, which track each other closely in amplitude and phase from dc to 12.4 GHz. The device to be measured is inserted in the test channel, as shown in Fig. 6. Variations in the physical length of test devices can be compensated for by a mechanical extension of the reference channel of the test unit. Thus the magnitude and phase of the transmission coefficient is measured with respect to a length of precision air-line. Of course gain- and phase-difference measurements between similar devices can also be made by inserting a device in each channel. Excess electrical

length in the test device can be compensated for by the line stretcher which acts as an extension to the electrical length of the reference channel.

Since the impedance levels in both reference and test channels are 50 ohms, the ratio of the voltage magnitudes applied to the test and reference channels of the harmonic frequency converter is proportional to the insertion gain (or loss),  $s_{12}$  or  $s_{21}$ , of the device with respect to the reference impedance 50 ohms. The phase between these voltages is likewise the insertion phase shift. When insertion parameters are being measured, the quantities of greatest interest are a logarithmic measure of gain (dB) and transfer phase shift. To obtain these quantities, the network analyzer is used with the phase-gain indicator plug-in.

### Reflection Measurements

Complex reflection coefficient, admittance, and impedance measurements are made using the set-up shown in Fig. 7. In this case the signal from the swept-frequency source drives a reflection test unit consisting of a dual directional coupler and a line stretcher. Only two reflection test units are needed to cover the analyzer's entire frequency range—one for frequencies between 0.11 and 2.0 GHz, and one for frequencies from 2.0 to 12.4 GHz.

For reflection measurements, the polar display plug-in with its built-in internal-graticule (parallax-free) CRT is most convenient. A Smith chart overlay for this display converts reflection coefficients directly to impedance or

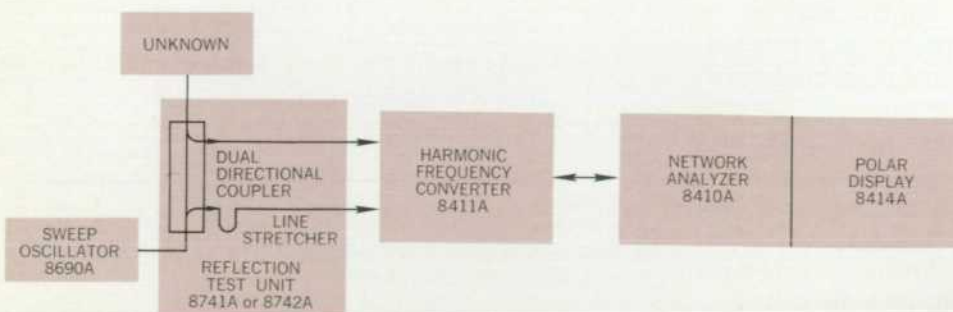


Fig. 7. Block diagram of reflection (impedance) test with new Network Analyzer.

Fig. 8. Model 8740A Transmission Test Unit or Models 8741A and 8742A Reflection Test Units contain the calibrated line stretchers, attenuators, and directional couplers needed for network analysis.



admittance. The line stretchers within the test units allow the plane at which the measurement is made to be extended past the connector to the unknown device. Thus the Smith Chart display can reveal the impedance or admittance within the test device as frequency is varied without the necessity of graphical manipulations of data plotted on a Smith chart. Seeing the impedance locus of a device over an octave-wide frequency range plotted on this display and watching it change as a tuning adjustment or some other condition is varied is truly an impressive experience for anyone who has ever had to use older methods.

#### Design considerations

In designing the new analyzer and in achieving some of its performance characteristics, several interesting circuit innovations were devised. Space limitations preclude a detailed treatment, but a summary of some of the salient innovations is given below.

- a. A wide-band phase-lock loop was designed to enable the system to sweep rapidly. Maximum sweep rate, which is determined by the loop bandwidth, is about 220 GHz per second.
- b. A voltage-controlled oscillator was devised to permit the harmonic frequency converter to tune over more than an octave in frequency (Fig. 9). With the varactors in Fig. 9 connected to the emitters, the voltage swings are small, permitting a low dc bias voltage to be used to get a large value of capacitance. Since the oscillator period is proportional to the varactor capacitance, a large tuning range results.
- c. The fast voltage-step needed to obtain fast sampling in the harmonic frequency converter is initiated in a step-recovery diode that operates in a 25-ohm line. To obtain a step of adequate voltage to accommodate the external sampled signal, it is necessary to drive this diode with substantial current. The current is provided by the basic power amplifier shown in Fig. 10. The amplifier follows the local oscillator and consists of emitter followers in a binary tree configuration. Each of the four output transistors supplies nearly 200 mA peak-to-peak over the range

from 60 to 150 MHz.

- d. In the IF circuits of the signal and reference channels of the main part of the analyzer, AGC action is required but with small relative amplitude and phase change between channels. To achieve this, AGC amplifiers were devised which remove up to 20 dB of power variation while giving less than 1 dB of differential amplitude change and less than about  $2^\circ$  of differential phase change. AGC action is obtained from the current-dependent incremental impedance characteristic of a silicon diode.
- e. Amplitude and phase change in the phase/gain in-

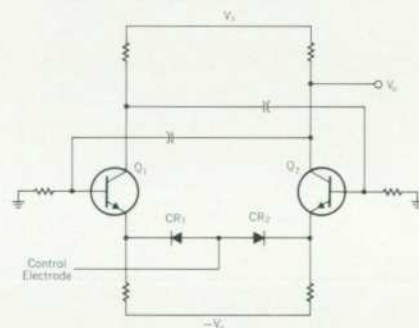


Fig. 9. Emitter-coupled multivibrator is used for voltage-controlled local oscillator. Tuning range is 60–150 MHz.

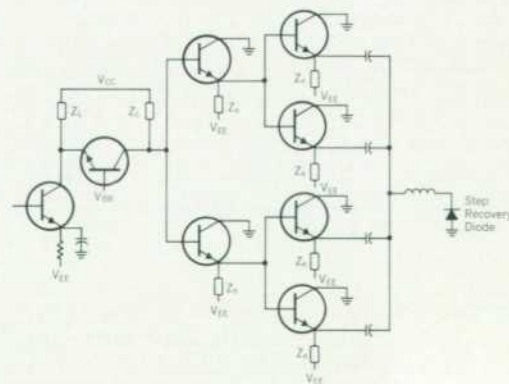


Fig. 10. Wide-band power amplifier provides at least 0.75 amp p-p over frequency range of 60–150 MHz.

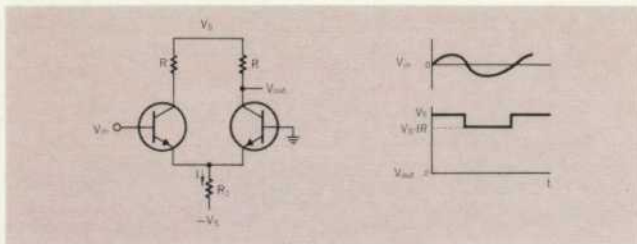


Fig. 11. Limiting amplifier with two transistors switching total current  $I$ . Output voltage is dependent only on  $V_s$  and  $R$ .

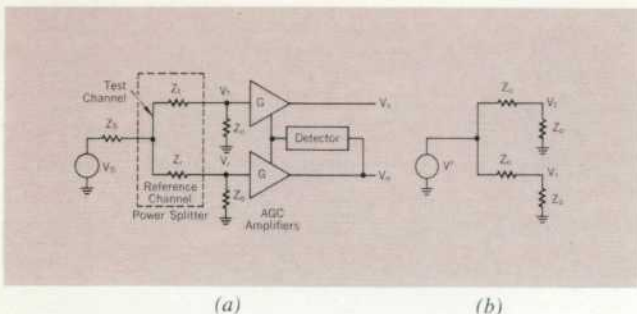
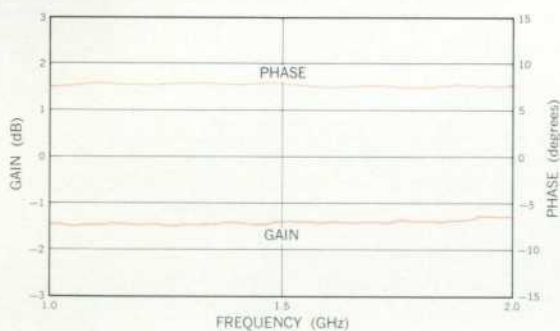
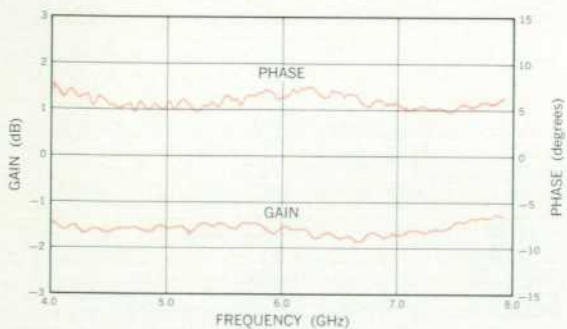


Fig. 12(a). Equivalent configuration of power divider and AGC amplifiers for calculating ratio. 12(b). Simplified equivalent with resultant zero-impedance source  $V'$ .



(a)



(b)

Fig. 13(a). Phase and gain responses typical of Network Analyzer between 1 GHz and 2 GHz: Analyzer is accurate within  $\pm 0.1$  dB and  $1.0^\circ$  in swept measurements. Accuracy in single-frequency measurements is better. (b). Phase and gain responses typical of Network Analyzer between 4 GHz and 8 GHz.

indicator unit were reduced by using a series of limiters of the type shown in Fig. 11. To prevent added delay when the amplifier starts to limit, the transistors are cut off but not allowed to saturate. A single limiter exhibits less than  $1^\circ$  of phase shift when passing from linear operation to limiting. Output voltage is dependent only on  $V_s$  and  $R$ .

- f. A major engineering contribution occurred in the form of two wide-band directional couplers used in the reflection test units. The couplers have 30 to 40 dB of directivity over their frequency ranges of 0.1 to 2 GHz and 2 to 12.4 GHz. This represents a combination of performance characteristics heretofore unattainable.
- g. Normally, a power divider operates with its three ports matched. In the transmission test unit a precision power divider was devised which operates with the source port matched but with the output ports mismatched. The ratio calculation performed by the AGC amplifiers (Fig. 12a) has the effect of making  $V'$  a low-impedance source, so that the two channels do not interact with each other. If  $Z_t$  and  $Z_r$  in Fig. 12(b) are made equal to  $Z_0$ , standing waves are not present.

## Performance

Typical measurement accuracies for the 1-to-2-GHz frequency range are shown in Fig. 13(a) which is a plot of the network analyzer's amplitude and phase responses over this range. Gain and phase measurements accurate within  $\pm 0.1$  dB and  $\pm 1^\circ$  appear reasonable for swept measurements. For single-frequency measurements, the accuracy is much better — comparable to that of standards-laboratory instruments.

Fig. 13(b) shows the amplitude and phase responses of the analyzer from 4 GHz to 8 GHz. The slightly-reduced calibration accuracy apparent in Fig. 13(b) can be attributed principally to the increased reflection coefficient of the harmonic frequency converter (wideband sampler) at higher frequencies.

Phase errors caused by changes in the amplitude of the signal in the test channel are shown in Fig. 14. Greatest accuracy in phase measurements is obtained for signal levels within  $\pm 20$  dB of mid-range. In this range, phase ambiguities are less than  $\pm 1^\circ$ .

Fig. 15 shows the gain and phase stability of the network analyzer. Over a period of six hours, total drift did not exceed 0.05 dB and  $0.2^\circ$  under normal room-temperature variations.

Gain and phase accuracies at low signal levels are limited by the signal-to-noise ratio at the output of the harmonic frequency converter. Noise in the test channel is below  $-80$  dBm, which means that accurate measure-

ments can be made for test-channel amplitudes down to  $-70$  dBm or less.

More typical measured data are presented in the s-parameter article (p. 13).

### Acknowledgments

It is a pleasure to acknowledge the contributions of the following members of the Microwave Division.

#### Network Analyzer Main Frame:

Kenneth S. Conroy, George M. Courreges, Wayne A. Fleming, Robert W. Pace.

#### Harmonic Frequency Converter:

William J. Benham, Richard T. Lee.

#### Phase/Gain Indicator Unit:

Donald G. Ferney, David R. Gildea, Alan L. Seely.

#### Polar Display Unit:

Larry L. Ritchie, William A. Rytand.

#### Transmission and Reflection Test Units:

Jean Pierre Castric, Wilmot B. Hunter, George R. Kirkpatrick, Richard A. Lyons, Auber G. Ryals.

#### Industrial Design:

Ned R. Kuypers.

We also wish to thank Microwave Division engineering manager Paul C. Ely, Jr. for his encouragement and helpful suggestions.

—Richard W. Anderson and  
Orthell T. Dennison

### REFERENCES

1. J. K. Hunton, and N. L. Pappas, 'The -hp- Microwave Reflectometers,' *'Hewlett-Packard Journal,'* Vol. 6, No. 1-2, Sept.-Oct. 1954.
2. P. D. Lacy, and D. E. Wheeler, 'A New 8-12 kMc Voltage-Tuned Sweep Oscillator for Faster Microwave Evaluations,' *'Hewlett-Packard Journal,'* Vol. 8, No. 6, Feb., 1957.
3. J. K. Hunton, and E. Lorence, 'Improved Sweep Frequency Techniques for Broad Band Microwave Testing,' *'Hewlett-Packard Journal,'* Vol. 12, No. 4, Dec., 1960.
4. S. B. Cohn, 'Microwave Automation,' *'the microwave journal,'* March, 1962, p. 13.
5. J. A. Young, 'Formula for Success,' *'the microwave journal,'* Feb., 1966, p. 58.

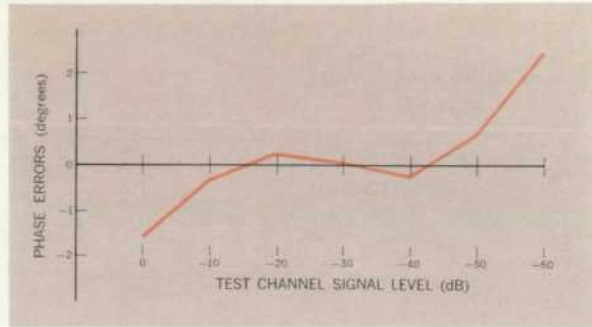


Fig. 14. Phase errors caused by changes in amplitude of signal in test channel are typically very small. Ambiguity is less than  $\pm 1^\circ$  for signals within  $\pm 20$  dB of mid-range.

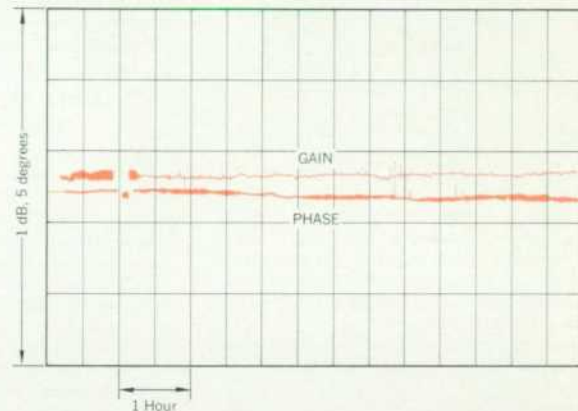


Fig. 15. Typical gain and phase stability of Network Analyzer. Total drift under normal room-temperature variations over six-hour period was  $< 0.05$  dB and  $< 0.2^\circ$ .



**Richard W. Anderson**

Dick Anderson joined the -hp- Microwave Division in 1959 after receiving his BSEE degree from Utah State University. He has contributed to the development of a variety of microwave instruments and devices, and he is now manager of the network analyzers section of the -hp- Microwave Laboratory. In 1963 he received his MS degree in electrical engineering from Stanford University on the -hp- Honors Cooperative Program.

Dick is active in the IEEE Group on Microwave Theory and Techniques. He holds several patents and has published a number of technical papers, his most recent being 'Sampler Based Instruments for Complex Signal and Network Analysis,' presented at WESCON 1966.



**Orthell T. Dennison**

Ted Dennison joined the -hp- Microwave Laboratory in 1960. He contributed to the design of the 415C and 415D SWR Meters, and directed the development of the 416B Ratio Meter and the later stages of the development of the 690-series Sweep Oscillators. Since 1963 he has been project leader of the 8410A Network Analyzer program.

Ted received his BSEE degree in 1960 from Utah State University and his MSEE degree in 1964 from the University of Santa Clara. At Santa Clara, he specialized in control systems and solid-state design. Ted is a member of IEEE, Sigma Tau, and Phi Kappa Phi.

## Condensed SPECIFICATIONS

-hp-

### 8410A Network Analyzer (Operating with 8411A)

**INSTRUMENT TYPE:** Measures relative amplitude and phase of two RF input signals; choice of two plug-in display modules for meter readout (8413A), or CRT polar display (8414A).

**FREQUENCY RANGE:** 0.11 to 12.4 GHz.

**TUNING:** Automatic over octave band selected by front panel switch.

**SWEEP OPERATION:** Sweeps in octave bands; apply sweep reference voltage for fast sweep operation (compatible with sweep reference out of Model 8690A Sweep Oscillators).

**INPUT IMPEDANCE:** 50 $\Omega$ ; SWR < 1.4 to 8 GHz, < 2.0 to 12.4 GHz; connectors precision 7mm coax.

**CHANNEL ISOLATION:** >70 dB, 0.11 to 6.0 GHz; >60 dB, to 12.4 GHz.

#### AMPLITUDE

##### INPUT POWER RANGE:

REFERENCE CHANNEL: -20 to -40 dBm ( $\pm 4$  dBm).

TEST CHANNEL: -10 ( $\pm 2$ ) dBm maximum. Not to exceed reference channel power by more than 10 dB.

##### DYNAMIC RANGE:

REFERENCE CHANNEL: 20 dB or more.

TEST CHANNEL: At least 60 dB.

**TEST CHANNEL NOISE:** Less than -78 dBm equivalent input noise (measured on 8413A Meter).

**AMPLITUDE CONTROL:** Adjusts gain of test channel relative to reference channel.

**RANGE:** 69 dB total in 10 and 1 dB steps; vernier provides continuous adjustment over at least 2 dB.

**ACCURACY:**  $\pm 0.1$  dB per 10 dB step, not to exceed  $\pm 0.2$  dB cumulative,  $\pm 0.05$  dB per 1 dB step, not to exceed  $\pm 0.1$  dB cumulative.

#### GENERAL

**PHASE CONTROL:** Vernier provides continuous phase reference adjustment over at least 90 $^\circ$ .

**OUTPUTS:** Two rear panel auxiliary outputs provide 278 kHz IF signals; outputs may be used for signal analysis, special applications, and convenient test points; modulation bandwidth nominally 10 kHz.

-hp-

### 8413A PHASE-GAIN INDICATOR (Installed in 8410A)

**INSTRUMENT TYPE:** Plug-in Meter display unit for 8410A. Displays relative amplitude in dB between reference and test channel inputs or relative phase in degrees. Pushbutton selection of meter function and range.

#### AMPLITUDE

**RANGE:**  $\pm 30$ , 10 and 3 dB full scale.

**ACCURACY:**  $\pm 3\%$  of end scale.

**LOG OUTPUT:** 50 millivolts per dB up to 60 dB total; bandwidth 10 kHz nominal depending on signal level; source impedance 1 k $\Omega$ ; accuracy,  $\pm 3\%$  of reading.

**LINEAR OUTPUT** (rear panel): 0 to 1 V maximum; 10 kHz bandwidth; 200 $\Omega$  source impedance.

##### MAXIMUM DRIFT:

LOG:  $\leq \pm 0.1$  dB per degree C.

LINEAR:  $\leq \pm 5$  mV per degree C.

#### PHASE

**RANGE:**  $\pm 180$ , 60, 18, 6 degrees full scale.

**ACCURACY:**  $\pm 2\%$  of end scale.

**OUTPUT:** 10 millivolts per degree; 10 kHz bandwidth; 1 k $\Omega$  source impedance. Accuracy  $\pm 2\%$  of reading.

**MAXIMUM DRIFT:**  $\pm 0.2$  degree per degree C.

**PHASE OFFSET:**  $\pm 180$  degrees in 10 degree steps.

**ACCURACY:**  $\pm 0.3$  degree per 10 degree step, not to exceed  $\pm 1.5$  degrees cumulative.

**PHASE RESPONSE VERSUS SIGNAL AMPLITUDE:** 4 degrees maximum phase change for 60 dB amplitude change in test channel.

-hp-

### 8414A POLAR DISPLAY (Installed in 8410A)

**INSTRUMENT TYPE:** Plug-in CRT display unit for 8410A. Displays amplitude and phase data in polar coordinates on 5" cathode ray tube.

**RANGE:** Normalized polar coordinate display; magnitude calibration 20% of full scale per division. Scale factor is a function of GAIN setting on 8410A. Maximum scale factor is 3.16 decreasing to at least 0.0316; phase calibrated in 10 $^\circ$  increments over 360 $^\circ$  range.

**ACCURACY:** Error circle on CRT <3 mm radius.

**OUTPUTS:** Two dc outputs provide horizontal and vertical components of polar quantity. Maximum output  $\pm 10$  volts, <100 $\Omega$  source impedance, bandwidth (3 dB) 10 kHz.

**DRIFT:** Beam center drift, <0.2 mm/ $^\circ$ C. Measurement drift, amplitude less than 2% of reading/ $^\circ$ C, phase less than 0.2 $^\circ$ / $^\circ$ C. Auxiliary outputs,  $\leq \pm 10$  mV/degree C.

**BEAM CENTER:** Pressing BEAM CENTER simulates zero-signal input to test channel. Allows convenient beam position adjustment for reference.

#### GENERAL

**CRT:** 5 inch, 5 kV post accelerator tube with P-2 phosphor; internal polar graticule.

**MARKER INPUT** (rear panel): Accepts frequency marker output pulse from -hp- 8690-Series and 690-Series Sweep Oscillators, -5 volts peak. Markers displayed as intensified dot on CRT display.

**BLANKING INPUT** (rear panel): Accepts -5 volt blanking pulse from -hp- 8690-Series and 690-Series Sweep Oscillators to blank retrace during swept operation.

**BACKGROUND ILLUMINATION:** Controls intensity of CRT background illumination for photography. Eliminates need for ultraviolet light source in oscilloscope camera when photographing internal graticule.

-hp-

### 8740A TRANSMISSION TEST UNIT

**INSTRUMENT TYPE:** RF power splitter and calibrated line stretcher for convenient transmission tests with 8410A. Provides reference and test channel RF outputs for connection to unknown device and the 8411A Converter.

**FREQUENCY RANGE:** dc to 12.4 GHz.

**FREQUENCY RESPONSE:** Reference and test channel outputs track a mean value within  $\pm 0.5$  dB amplitude and  $\pm 3$  degrees phase to 8.0 GHz;  $\pm 0.75$  dB and  $\pm 5$  degrees to 12.4 GHz (includes frequency response of 8411A Converter).

**OUTPUT IMPEDANCE:** 50 ohms, reflection coefficient 0.07 (1.15 SWR, 23 dB return loss) dc to 8 GHz; 0.11 (1.25 SWR, 19 dB return loss) 8.0 to 12.4 GHz.

##### REFERENCE PLANE EXTENSION:

Electrical; 0 to 30 centimeters.

Mechanical; 0 to 10 centimeters.

Both extensions calibrated by digital indicators.

-hp-

### 8414A AND 8742A REFLECTION TEST UNITS

**INSTRUMENT TYPE:** Wideband reflectometer, phase-balanced for swept or spot frequency impedance tests with 8410A. Calibrated variable reference plane.

**FREQUENCY RANGE:** 0.11 to 2.0 GHz (8741A); 2.0 to 12.4 GHz (8742A).

**FREQUENCY RESPONSE:** Incident and reflected outputs from reflectometer track a mean value within  $\pm 0.5$  dB amplitude,  $\pm 3$  degrees phase (8741A);  $\pm 0.75$  dB,  $\pm 5$  degrees over any octave (8742A) (includes frequency response of 8411A Converter).

**IMPEDANCE:** 50 ohms.

**RESIDUAL REFLECTION COEFFICIENT:** <0.01, 0.11 to 1.0 GHz; <0.02, 1.0 to 2.0 GHz (8741A); <0.03, 2.0 to 12.4 GHz (8742A).

**REFERENCE PLANE EXTENSION:** 0 to 15 cm (8741A); 0 to 17 cm (8742A); calibrated by digital dial indicator.

**PRICES:** 8410A \$1700; 8411A \$2200; 8413A \$825; 8414A \$825; 8740A \$1100; 8741A and 8742A less than \$1500 each.

##### MANUFACTURING DIVISION:

-hp- Microwave Division

1501 Page Mill Road

Palo Alto, California 94304

Prices f.o.b. factory

Data subject to change without notice

# The Engineer, Automated Network Analysis and the Computer – Signs of Things to Come

**T**HREE NEW DEVELOPMENTS hold exciting possibilities for microwave measurement and design. The new developments referred to are the Network Analyzer (p. 2), the new design procedures using scattering parameters (p. 13), and an unusual new instrumentation computer recently developed by the -hp- Dymec division. The Analyzer and the s-parameter design procedures are new tools that can logically and analytically solve problems that until now had to be attacked empirically. The instrumentation computer can magnify the power and potential of these tools manyfold. Combined as tomorrow's instrument system, they offer the microwave engineer capabilities he has never had before.

To show the implications for other future instrumentation systems, we will trace the history of these three developments in our laboratory and look at the prototype system evolving therefrom.

The Network Analyzer project started several years ago with some basic ideas fortified by intuition but with little information about the increasing importance of its applications. During the course of the Analyzer project, the development of a related instrument, the RF Vector Voltmeter,<sup>1</sup> was completed, and several of our engineers found that with it their efforts to advance high-frequency solid-state circuit performance were helped by using the scattering-parameter characterization of the active devices. The scattering-parameter design procedures<sup>2</sup> evolved from these first measurements.

After a time, when the first prototypes of the new Network Analyzer were completed, they were pressed into service measuring active devices in chip form and thin-film components for our hybrid microcircuits. These measurements were coupled with the newly-evolved design procedures and resulted in several important advances in high-frequency integrated circuits.

As the s-parameter design techniques were applied to increasingly difficult problems, it became apparent that

the design calculations and transformations could be carried out to advantage by computer. Programs were developed on the B-5500 computer at the nearby Stanford Computational Center used by our engineers. The results were quite rewarding. Later, when a computer time-share terminal was installed in the lab, several shorter programs were written and we found that the direct link between the computer and the engineer offered many advantages.

## Computerized HF Transistor Measurement

The next step was obvious: as we began to think about using the newly developed instrumentation computer, we became more and more enthusiastic about the possibilities of combining the three developments. These concepts have grown until we are now evaluating the prototype system shown in the diagram. The prototype system consists of a 0.1 to 2 Gc programmable source, the 8410 Network Analyzer system, a prototype transducer instrument for transistor parameter measurement, programmable transistor bias supplies and the 2116 Instrumentation Computer. The computer controls all the conditions of measurements including test frequency, transistor bias, and the parameter to be measured. The transistor itself is inserted in a removable fixture which can be adapted to any transistor package configuration. The 8410 Network Analyzer reads into the computer through a digital voltmeter.

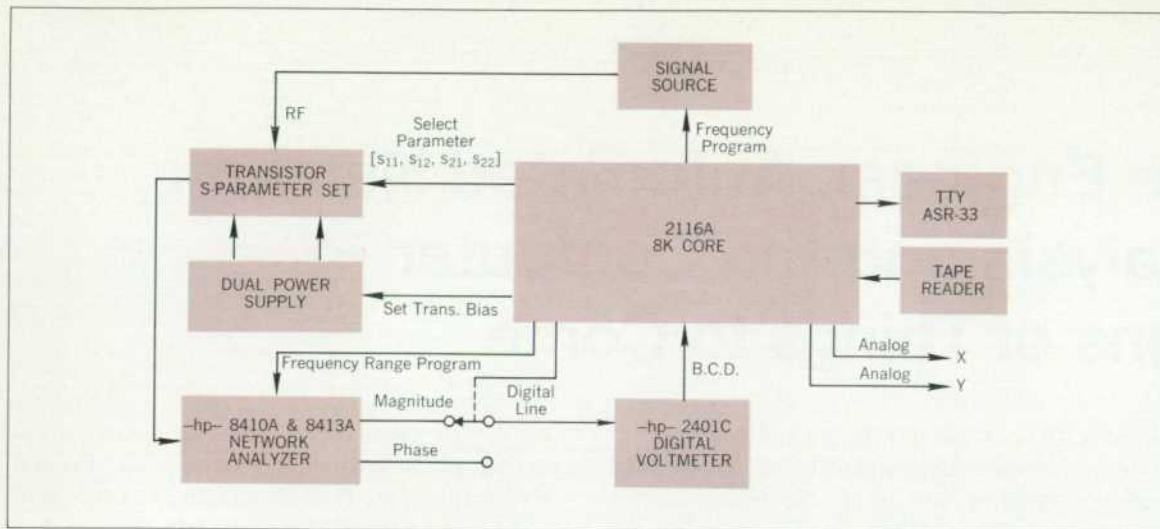
A not insignificant advantage of the use of a computer in this system is the capability to correct measurement errors. The system is first calibrated with unity and zero s-parameter standards. The computer calculates and stores the error vector for each frequency and as the data is taken it subtracts out these values. The accuracy and dynamic range of measurement are greatly improved by this procedure.

In operation the engineer can select one or a number of frequencies and bias conditions and can ask the computer to do a variety of operations such as:

1. Measure and correct the s-parameters.
2. Convert to h, y, or z-parameters.

<sup>1</sup> Fritz K. Weinert, 'The RF Vector Voltmeter — an Important New Instrument for Amplitude and Phase Measurements from 1 MHz to 1000 MHz,' *Hewlett-Packard Journal*, Vol. 17, No. 9, May, 1966.

<sup>2</sup> George E. Bodway, 'Two-Port Power Flow Analysis of Linear Active Circuits Using the Generalized Scattering Parameters,' Hewlett-Packard Company Internal Report.



3. Calculate maximum available power gain  $G_{A \max}$ .
4. Calculate the terminal conditions to achieve  $G_{A \max}$ .
5. Find gain-bandwidth product  $f_t$ .
6. Find maximum frequency of oscillation  $f_{\max}$ .
7. Find the biases for maximum  $f_t$  and for  $f_{\max}$ .

The engineer communicates with the system through a typewriter and the computer control panel.

The programs are being improved to incorporate additional design analysis calculations and eventually some

network synthesis operations. Several other organizations are working on computer-aided circuit design for high frequency applications. Bell Telephone Laboratories and Texas Instruments, for example, have particularly significant efforts in these areas. We can look for many advances in the design and synthesis techniques as this work proceeds. However, the concept as it has been developing at HP is somewhat unusual in that the experimental measurements, and the design computations are combined in one on-line system controlled directly by the engineer. The man-machine communication is in the normal language the engineer uses to solve these problems.

### Future Measurement Systems

The possibilities for this instrument system to add significantly to the power of our engineers are impressive. But beyond the value of this particular system are the implications for the whole field of high frequency instrumentation. It is easy to imagine a number of measurement systems using the on-line computer to provide new and valuable capabilities. The computer and the rest of the system combine to form a new instrument of greatly magnified capabilities, particularly if the man-machine interface is also designed for the specific function of this new instrument. We can look for several levels of microwave instrumentation systems: some will just control the measurement and perhaps correct the data; others will go on to analyze the data; the most sophisticated will carry on from the analysis into synthesis operations.

These beguiling concepts offer the opportunities for many new contributions in instrumentation developments at Hewlett-Packard and our engineers are approaching these opportunities with enthusiasm.

— Paul C. Ely, Jr.

**Paul C. Ely, Jr.**



Paul Ely has been active in the microwave and radar instrumentation field for fifteen years. At -hp-, Paul has been associated with the development of the -hp- 690 series sweep oscillators as well as with microwave spectroscopy work, and was section manager of the group that did the early development work on the 8410 Network Analyzer discussed in this issue. At present he is engineering manager for the -hp- Microwave Division laboratory.

Paul holds a BS in Engineering Physics from Lehigh University and received a MS in EE from Stanford University under the -hp- Honors Co-op Plan. He is active in IEEE work, having served on national and sectional committees. Presently he is secretary-treasurer of the IEEE PG on Instrumentation and Measurement and is a director of the San Francisco Bay Area Science Fair.

# S-Parameter Techniques for Faster, More Accurate Network Design

**L**INEAR NETWORKS, OR NONLINEAR NETWORKS operating with signals sufficiently small to cause the networks to respond in a linear manner, can be completely characterized by parameters measured at the network terminals (ports) without regard to the contents of the networks. Once the parameters of a network have been determined, its behavior in any external environment can be predicted, again without regard to the specific contents of the network. The new microwave network analyzer described in the article beginning on p. 2 characterizes networks by measuring one kind of parameters, the scattering parameters, or s-parameters.

S-parameters are being used more and more in microwave design because they are easier to measure and work with at high frequencies than other kinds of parameters. They are conceptually simple, analytically convenient, and capable of providing a surprising degree of insight into a measurement or design problem. For these reasons, manufacturers of high-frequency transistors and other solid-state devices are finding it more meaningful to specify their products in terms of s-parameters than in any other way. How s-parameters can simplify microwave design problems, and how a designer can best take advantage of their abilities, are described in this article.

## Two-Port Network Theory

Although a network may have any number of ports, network parameters can be explained most easily by considering a network with only two ports, an input port and an output port, like the network shown in Fig. 1. To characterize the performance of such a network, any of several parameter sets can be used, each of which has certain advantages.

Each parameter set is related to a set of four variables associated with the two-port model. Two of these variables represent the excitation of the network (independent variables), and the remaining two represent the response of the network to the excitation (dependent variables). If the network of Fig. 1 is excited by voltage sources  $V_1$  and  $V_2$ , the

network currents  $I_1$  and  $I_2$  will be related by the following equations (assuming the network behaves linearly):

$$I_1 = y_{11}V_1 + y_{12}V_2 \quad (1)$$

$$I_2 = y_{21}V_1 + y_{22}V_2 \quad (2)$$

In this case, with port voltages selected as independent variables and port currents taken as dependent variables, the relating parameters are called short-circuit admittance parameters, or y-parameters. In the absence of additional information, four measurements are required to determine the four parameters  $y_{11}$ ,  $y_{21}$ ,  $y_{12}$ , and  $y_{22}$ . Each measurement is made with one port of the network excited by a voltage source while the other port is short circuited. For example,  $y_{21}$ , the forward transadmittance, is the ratio of the current at port 2 to the voltage at port 1 with port 2 short circuited as shown in equation 3.

$$y_{21} = \frac{I_2}{V_1} \Big|_{V_2 = 0} \text{ (output short circuited)} \quad (3)$$

If other independent and dependent variables had been chosen, the network would have been described, as before, by two linear equations similar to equations 1 and 2, except that the variables and the parameters describing their relationships would be different. However, all parameter sets contain the same information about a network, and it is always possible to calculate any set in terms of any other set.

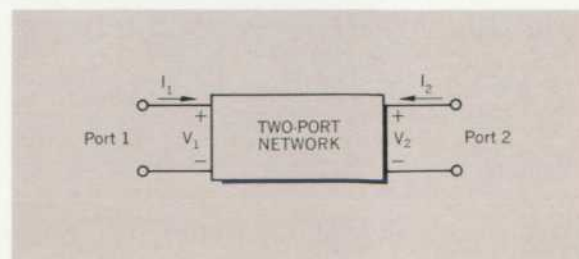


Fig. 1. General two-port network.

## S-Parameters

The ease with which scattering parameters can be measured makes them especially well suited for describing transistors and other active devices. Measuring most other parameters calls for the input and output of the device to be successively opened and short circuited. This is difficult to do even at RF frequencies where lead inductance and capacitance make short and open circuits difficult to obtain. At higher frequencies these measurements typically require tuning stubs, separately adjusted at each measurement frequency, to reflect short or open circuit conditions to the device terminals. Not only is this inconvenient and tedious, but a tuning stub shunting the input or output may cause a transistor to oscillate, making the measurement difficult and invalid. S-parameters, on the other hand, are usually measured with the device imbedded between a 50Ω load and source, and there is very little chance for oscillations to occur.

Another important advantage of s-parameters stems from the fact that traveling waves, unlike terminal voltages and currents, do not vary in magnitude at points along a lossless transmission line. This means that scattering parameters can be measured on a device located at some distance from the measurement transducers, provided that the measuring device and the transducers are connected by low-loss transmission lines.

Generalized scattering parameters have been defined by K. Kurokawa.<sup>1</sup> These parameters describe the interrelationships of a new set of variables ( $a_1$ ,  $b_1$ ). The variables  $a_1$  and  $b_1$  are normalized complex voltage waves incident on and reflected from the  $i^{\text{th}}$  port of the network. They are defined in terms of the terminal voltage  $V_i$ , the terminal current  $I_i$ , and an arbitrary reference impedance  $Z_i$ , as follows

<sup>1</sup> K. Kurokawa, 'Power Waves and the Scattering Matrix,' IEEE Transactions on Microwave Theory and Techniques, Vol. MTT-13, No. 2, March, 1965.

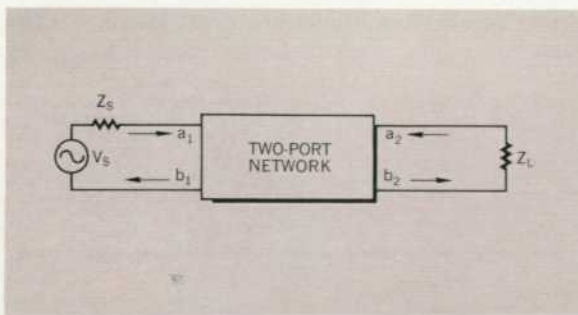


Fig. 2. Two-port network showing incident ( $a_1$ ,  $a_2$ ) and reflected ( $b_1$ ,  $b_2$ ) waves used in s-parameter definitions.

$$a_i = \frac{V_i + Z_i I_i}{2\sqrt{\text{Re } Z_i}} \quad (4)$$

$$b_i = \frac{V_i - Z_i^* I_i}{2\sqrt{\text{Re } Z_i}} \quad (5)$$

where the asterisk denotes the complex conjugate.

For most measurements and calculations it is convenient to assume that the reference impedance  $Z_i$  is positive and real. For the remainder of this article, then, all variables and parameters will be referenced to a single positive real impedance  $Z_0$ .

The wave functions used to define s-parameters for a two-port network are shown in Fig. 2. The independent variables  $a_1$  and  $a_2$  are normalized incident voltages, as follows:

$$a_1 = \frac{V_1 + I_1 Z_0}{2\sqrt{Z_0}} = \frac{\text{voltage wave incident on port 1}}{\sqrt{Z_0}} = \frac{V_{11}}{\sqrt{Z_0}} \quad (6)$$

$$a_2 = \frac{V_2 + I_2 Z_0}{2\sqrt{Z_0}} = \frac{\text{voltage wave incident on port 2}}{\sqrt{Z_0}} = \frac{V_{12}}{\sqrt{Z_0}} \quad (7)$$

Dependent variables  $b_1$  and  $b_2$  are normalized reflected voltages:

$$b_1 = \frac{V_1 - I_1 Z_0}{2\sqrt{Z_0}} = \frac{\text{voltage wave reflected (or emanating) from port 1}}{\sqrt{Z_0}} = \frac{V_{r1}}{\sqrt{Z_0}} \quad (8)$$

$$b_2 = \frac{V_2 - I_2 Z_0}{2\sqrt{Z_0}} = \frac{\text{voltage wave reflected (or emanating) from port 2}}{\sqrt{Z_0}} = \frac{V_{r2}}{\sqrt{Z_0}} \quad (9)$$

The linear equations describing the two-port network are then:

$$b_1 = s_{11} a_1 + s_{12} a_2 \quad (10)$$

$$b_2 = s_{21} a_1 + s_{22} a_2 \quad (11)$$

The s-parameters  $s_{11}$ ,  $s_{22}$ ,  $s_{21}$ , and  $s_{12}$  are:

$$s_{11} = \left. \frac{b_1}{a_1} \right|_{a_2=0} = \text{Input reflection coefficient with the output port terminated by a matched load } (Z_L = Z_0 \text{ sets } a_2 = 0). \quad (12)$$

$$s_{22} = \left. \frac{b_2}{a_2} \right|_{a_1=0} = \text{Output reflection coefficient with the input terminated by a matched load } (Z_S = Z_0 \text{ and } V_S = 0). \quad (13)$$

$$s_{21} = \left. \frac{b_2}{a_1} \right|_{a_2=0} = \text{Forward transmission (insertion) gain with the output port terminated in a matched load.} \quad (14)$$

$$s_{12} = \left. \frac{b_1}{a_2} \right|_{a_1=0} = \text{Reverse transmission (insertion) gain with the input port terminated in a matched load.} \quad (15)$$

Notice that

$$s_{11} = \frac{b_1}{a_1} = \frac{\frac{V_1}{I_1} - Z_0}{\frac{V_1}{I_1} + Z_0} = \frac{Z_1 - Z_0}{Z_1 + Z_0} \quad (16)$$

$$\text{and} \quad Z_1 = Z_0 \frac{(1 + s_{11})}{(1 - s_{11})} \quad (17)$$

where  $Z_1 = \frac{V_1}{I_1}$  is the input impedance at port 1.

This relationship between reflection coefficient and impedance is the basis of the Smith Chart transmission-line calculator. Consequently, the reflection coefficients  $s_{11}$  and  $s_{22}$  can be plotted on Smith charts, converted directly to impedance, and easily manipulated to determine matching networks for optimizing a circuit design.

The above equations show one of the important advantages of s-parameters, namely that they are simply gains and reflection coefficients, both familiar quantities to engineers. By comparison, some of the y-parameters described earlier in this article are not so familiar. For example, the y-parameter corresponding to insertion gain  $s_{21}$  is the 'forward transadmittance'  $y_{21}$  given by equation 3. Clearly, insertion gain gives by far the greater insight into the operation of the network.

Another advantage of s-parameters springs from the simple relationships between the variables  $a_1$ ,  $a_2$ ,  $b_1$ , and  $b_2$ , and various power waves:

$$|a_1|^2 = \text{Power incident on the input of the network.} \\ = \text{Power available from a source of impedance } Z_0.$$

$$|a_2|^2 = \text{Power incident on the output of the network.} \\ = \text{Power reflected from the load.}$$

$$|b_1|^2 = \text{Power reflected from the input port of the network.} \\ = \text{Power available from a } Z_0 \text{ source minus the power delivered to the input of the network.}$$

$$|b_2|^2 = \text{Power reflected or emanating from the output of the network.} \\ = \text{Power incident on the load.} \\ = \text{Power that would be delivered to a } Z_0 \text{ load.}$$

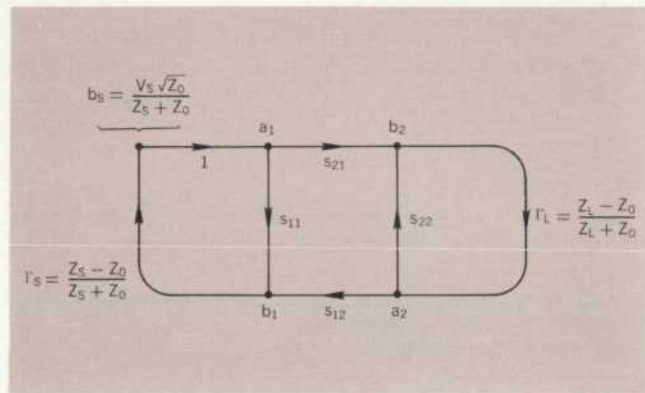


Fig. 3. Flow graph of network of Fig. 2.

Hence s-parameters are simply related to power gain and mismatch loss, quantities which are often of more interest than the corresponding voltage functions:

$$|s_{11}|^2 = \frac{\text{Power reflected from the network input}}{\text{Power incident on the network input}}$$

$$|s_{22}|^2 = \frac{\text{Power reflected from the network output}}{\text{Power incident on the network output}}$$

$$|s_{21}|^2 = \frac{\text{Power delivered to a } Z_0 \text{ load}}{\text{Power available from } Z_0 \text{ source}} \\ = \text{Transducer power gain with } Z_0 \text{ load and source}$$

$$|s_{12}|^2 = \text{Reverse transducer power gain with } Z_0 \text{ load and source.}$$

### Network Calculations with Scattering Parameters

Scattering parameters turn out to be particularly convenient in many network calculations. This is especially true for power and power gain calculations. The transfer parameters  $s_{12}$  and  $s_{21}$  are a measure of the complex insertion gain, and the driving point parameters  $s_{11}$  and  $s_{22}$  are a measure of the input and output mismatch loss. As dimensionless expressions of gain and reflection, the parameters not only give a clear and meaningful physical interpretation of the network

performance but also form a natural set of parameters for use with signal flow graphs<sup>2,3</sup>. Of course, it is not necessary to use signal flow graphs in order to use s-parameters, but flow graphs make s-parameter calculations extremely simple, and I recommend them very strongly. Flow graphs will be used in the examples that follow.

In a signal flow graph each port is represented by two nodes. Node  $a_n$  represents the wave coming into the device from another device at port  $n$  and node  $b_n$  represents the wave leaving the device at port  $n$ . The complex scattering coefficients are then represented as multipliers on branches connecting the nodes within the network and in adjacent networks. Fig. 3 is the flow graph representation of the system of Fig. 2.

Fig. 3 shows that if the load reflection coefficient  $\Gamma_L$  is zero ( $Z_L = Z_0$ ) there is only one path connecting  $b_1$  to  $a_1$  (flow graph rules prohibit signal flow against the forward direction of a branch arrow). This confirms the definition of  $s_{11}$ :

$$s_{11} = \left. \frac{b_1}{a_1} \right|_{a_2 = \Gamma_L b_2 = 0}$$

The simplification of network analysis by flow graphs results from the application of the "non-touching loop rule." This rule applies a generalized formula to determine the transfer function between any two nodes within a complex system. The non-touching loop rule is explained in footnote 4.

<sup>2</sup> J. K. Hunton, 'Analysis of Microwave Measurement Techniques by Means of Signal Flow Graphs,' IRE Transactions on Microwave Theory and Techniques, Vol. MTT-8, No. 2, March, 1960.

<sup>3</sup> N. Kuhn, 'Simplified Signal Flow Graph Analysis,' Microwave Journal, Vol. 6, No. 11, Nov., 1963.

<sup>4</sup> The nontouching loop rule provides a simple method for writing the solution of any flow graph by inspection. The solution  $T$  (the ratio of the output variable to the input variable) is

$$T = \frac{\sum_k T_k \Delta_k}{\Delta}$$

where  $T_k$  = path gain of the  $k^{\text{th}}$  forward path

$\Delta = 1 - (\text{sum of all individual loop gains}) + (\text{sum of the loop gain products of all possible combinations of two nontouching loops}) - (\text{sum of the loop gain products of all possible combinations of three nontouching loops}) + \dots$

$\Delta_k$  = The value of  $\Delta$  not touching the  $k^{\text{th}}$  forward path.

A path is a continuous succession of branches, and a forward path is a path connecting the input node to the output node, where no node is encountered more than once. Path gain is the product of all the branch multipliers along the path. A loop is a path which originates and terminates on the same node, no node being encountered more than once. Loop gain is the product of the branch multipliers around the loop.

For example, in Fig. 3 there is only one forward path from  $b_5$  to  $b_2$  and its gain is  $s_{21}$ . There are two paths from  $b_5$  to  $b_1$ ; their path gains are  $s_{21}s_{12}\Gamma_L$  and  $s_{11}$ , respectively. There are three individual loops, only one combination of two nontouching loops, and no combinations of three or more nontouching loops; therefore, the value of  $\Delta$  for this network is

$$\Delta = 1 - (s_{11}\Gamma_S + s_{21}s_{12}\Gamma_L\Gamma_S + s_{22}\Gamma_L) + (s_{11}s_{22}\Gamma_L\Gamma_S)$$

The transfer function from  $b_5$  to  $b_2$  is therefore

$$\frac{b_2}{b_5} = \frac{s_{21}}{\Delta}$$

Using scattering parameter flow-graphs and the non-touching loop rule, it is easy to calculate the transducer power gain with arbitrary load and source. In the following equations the load and source are described by their reflection coefficients  $\Gamma_L$  and  $\Gamma_S$ , respectively, referenced to the real characteristic impedance  $Z_0$ .

Transducer power gain

$$G_T = \frac{\text{Power delivered to the load}}{\text{Power available from the source}} = \frac{P_L}{P_{avs}}$$

$$P_L = P(\text{incident on load}) - P(\text{reflected from load})$$

$$= |b_2|^2 (1 - |\Gamma_L|^2)$$

$$P_{avs} = \frac{|b_s|^2}{(1 - |\Gamma_S|^2)}$$

$$G_T = \left| \frac{b_2}{b_s} \right|^2 (1 - |\Gamma_S|^2) (1 - |\Gamma_L|^2)$$

Using the non-touching loop rule,

$$\frac{b_2}{b_s} = \frac{s_{21}}{1 - s_{11}\Gamma_S - s_{22}\Gamma_L - s_{21}s_{12}\Gamma_L\Gamma_S + s_{11}\Gamma_S s_{22}\Gamma_L}$$

$$= \frac{s_{21}}{(1 - s_{11}\Gamma_S)(1 - s_{22}\Gamma_L) - s_{21}s_{12}\Gamma_L\Gamma_S}$$

$$G_T = \frac{|s_{21}|^2 (1 - |\Gamma_S|^2) (1 - |\Gamma_L|^2)}{|(1 - s_{11}\Gamma_S)(1 - s_{22}\Gamma_L) - s_{21}s_{12}\Gamma_L\Gamma_S|^2} \quad (18)$$

Two other parameters of interest are:

1) Input reflection coefficient with the output termination arbitrary and  $Z_S = Z_0$ .

$$s'_{11} = \frac{b_1}{a_1} = \frac{s_{11}(1 - s_{22}\Gamma_L) + s_{21}s_{12}\Gamma_L}{1 - s_{22}\Gamma_L}$$

$$= s_{11} + \frac{s_{21}s_{12}\Gamma_L}{1 - s_{22}\Gamma_L} \quad (19)$$

2) Voltage gain with arbitrary source and load impedances

$$A_V = \frac{V_2}{V_1} \quad V_1 = (a_1 + b_1) \sqrt{Z_0} = V_{11} + V_{r1}$$

$$V_2 = (a_2 + b_2) \sqrt{Z_0} = V_{12} + V_{r2}$$

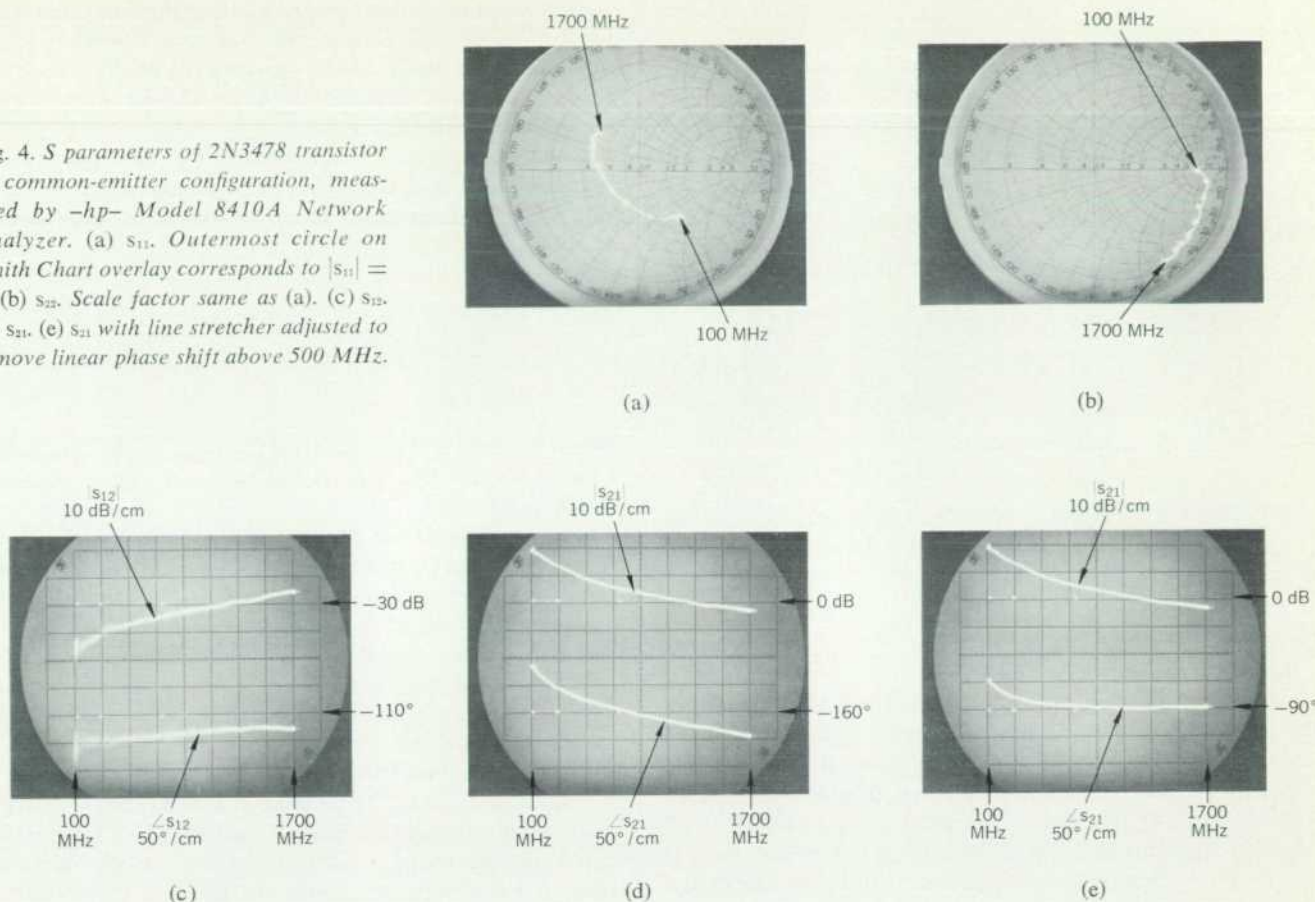
$$a_2 = \Gamma_L b_2$$

$$b_1 = s'_{11} a_1$$

$$A_V = \frac{b_2(1 + \Gamma_L)}{a_1(1 + s'_{11})} = \frac{s_{21}(1 + \Gamma_L)}{(1 - s_{22}\Gamma_L)(1 + s'_{11})} \quad (20)$$

On p. 23 is a table of formulas for calculating many often-used network functions (power gains, driving point characteristics, etc.) in terms of scattering parameters. Also included in the table are conversion formulas between s-parameters and h-, y-, and z-parameters, which are other parameter sets used very often for specifying transistors at

Fig. 4. *S* parameters of 2N3478 transistor in common-emitter configuration, measured by *hp*- Model 8410A Network Analyzer. (a)  $s_{11}$ . Outermost circle on Smith Chart overlay corresponds to  $|s_{11}| = 1$ . (b)  $s_{22}$ . Scale factor same as (a). (c)  $s_{12}$ . (d)  $s_{21}$ . (e)  $s_{21}$  with line stretcher adjusted to remove linear phase shift above 500 MHz.



lower frequencies. Two important figures of merit used for comparing transistors,  $f_t$  and  $f_{max}$ , are also given, and their relationship to *s*-parameters is indicated.

#### Amplifier Design Using Scattering Parameters

The remainder of this article will show by several examples how *s*-parameters are used in the design of transistor amplifiers and oscillators. To keep the discussion from becoming bogged down in extraneous details, the emphasis in these examples will be on *s*-parameter design methods, and mathematical manipulations will be omitted wherever possible.

#### Measurement of S-Parameters

Most design problems will begin with a tentative selection of a device and the measurement of its *s*-parameters. Fig. 4 is a set of oscillograms containing complete *s*-parameter data for a 2N3478 transistor in the common-emitter configuration. These oscillograms are the results of swept-frequency measurements made with the new microwave network analyzer described elsewhere in this issue. They represent the actual *s*-parameters of this transistor between 100 MHz and 1700 MHz.

In Fig. 5, the magnitude of  $s_{21}$  from Fig. 4(d) is replotted on a logarithmic frequency scale, along with additional data on  $s_{21}$  below 100 MHz, measured with a vector voltmeter. The magnitude of  $s_{21}$  is essentially constant to 125 MHz, and then rolls off at a slope of 6 dB/octave. The phase angle

of  $s_{21}$ , as seen in Fig. 4(d), varies linearly with frequency above about 500 MHz. By adjusting a calibrated line stretcher in the network analyzer, a compensating linear phase shift was introduced, and the phase curve of Fig. 4(e) resulted. To go from the phase curve of Fig. 4(d) to that of Fig. 4(e) required 3.35 cm of line, equivalent to a pure time delay of 112 picoseconds.

After removal of the constant-delay, or linear-phase, component, the phase angle of  $s_{21}$  for this transistor [Fig. 4(e)] varies from  $0^\circ$  at dc to  $-90^\circ$  at high frequencies, passing through  $-45^\circ$  at 125 MHz, the  $-3$  dB point of the magnitude curve. In other words,  $s_{21}$  behaves like a single pole in the frequency domain, and it is possible to write a closed expression for it. This expression is

$$s_{21} = \frac{s_{210} e^{-j\omega T_0}}{1 + j\frac{\omega}{\omega_0}} \quad (21)$$

where

$$T_0 = 112 \text{ ps}$$

$$\omega = 2\pi f$$

$$\omega_0 = 2\pi \times 125 \text{ MHz}$$

$$s_{210} = 11.2 = 21 \text{ dB}$$

The time delay  $T_0 = 112$  ps is due primarily to the transit time of minority carriers (electrons) across the base of this npn transistor.

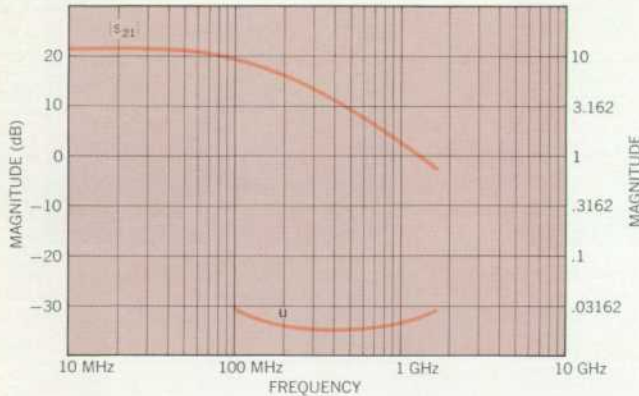


Fig. 5. Top curve:  $|s_{21}|$  from Fig. 4 replotted on logarithmic frequency scale. Data below 100 MHz measured with *hp-8405A* Vector Voltmeter. Bottom curve: unilateral figure of merit, calculated from *s* parameters (see text).

### Narrow-Band Amplifier Design

Suppose now that this 2N3478 transistor is to be used in a simple amplifier, operating between a  $50\Omega$  source and a  $50\Omega$  load, and optimized for power gain at 300 MHz by means of lossless input and output matching networks. Since reverse gain  $s_{12}$  for this transistor is quite small — 50 dB smaller than forward gain  $s_{21}$ , according to Fig. 4 — there is a possibility that it can be neglected. If this is so, the design problem will be much simpler, because setting  $s_{12}$  equal to zero will make the design equations much less complicated.

In determining how much error will be introduced by assuming  $s_{12} = 0$ , the first step is to calculate the unilateral figure of merit  $u$ , using the formula given in the table on p. 23, i.e.

$$u = \frac{|s_{11}s_{12}s_{21}s_{22}|}{(1 - |s_{11}|^2)(1 - |s_{22}|^2)} \quad (22)$$

A plot of  $u$  as a function of frequency, calculated from the measured parameters, appears in Fig. 5. Now if  $G_{Tu}$  is the transducer power gain with  $s_{12} = 0$  and  $G_T$  is the actual transducer power gain, the maximum error introduced by using  $G_{Tu}$  instead of  $G_T$  is given by the following relationship:

$$\frac{1}{(1 + u)^2} < \frac{G_T}{G_{Tu}} < \frac{1}{(1 - u)^2} \quad (23)$$

From Fig. 5, the maximum value of  $u$  is about 0.03, so the maximum error in this case turns out to be about  $\pm 0.25$  dB at 100 MHz. This is small enough to justify the assumption that  $s_{12} = 0$ .

Incidentally, a small reverse gain, or feedback factor,  $s_{12}$ , is an important and desirable property for a transistor to have, for reasons other than that it simplifies amplifier de-

sign. A small feedback factor means that the input characteristics of the completed amplifier will be independent of the load, and the output will be independent of the source impedance. In most amplifiers, isolation of source and load is an important consideration.

Returning now to the amplifier design, the unilateral expression for transducer power gain, obtained either by setting  $s_{12} = 0$  in equation 18 or by looking in the table on p. 23, is

$$G_{Tu} = \frac{|s_{21}|^2(1 - |\Gamma_S|^2)(1 - |\Gamma_L|^2)}{|1 - s_{11}\Gamma_S|^2|1 - s_{22}\Gamma_L|^2} \quad (24)$$

When  $|s_{11}|$  and  $|s_{22}|$  are both less than one, as they are in this case, maximum  $G_{Tu}$  occurs for  $\Gamma_S = s_{11}^*$  and  $\Gamma_L = s_{22}^*$  (table, p. 23).

The next step in the design is to synthesize matching networks which will transform the  $50\Omega$  load and source impedances to the impedances corresponding to reflection coefficients of  $s_{11}^*$  and  $s_{22}^*$ , respectively. Since this is to be a single-frequency amplifier, the matching networks need not be complicated. Simple series-capacitor, shunt-inductor networks will not only do the job, but will also provide a handy means of biasing the transistor — via the inductor — and of isolating the dc bias from the load and source.

Values of  $L$  and  $C$  to be used in the matching networks are determined using the Smith Chart of Fig. 6. First, points corresponding to  $s_{11}$ ,  $s_{11}^*$ ,  $s_{22}$ , and  $s_{22}^*$  at 300 MHz are plotted. Each point represents the tip of a vector leading away from the center of the chart, its length equal to the magnitude of the reflection coefficient being plotted, and its angle equal to the phase of the coefficient. Next, a combination of constant-resistance and constant-conductance circles is found, leading from the center of the chart, representing  $50\Omega$ , to  $s_{11}^*$  and  $s_{22}^*$ . The circles on the Smith Chart are constant-resistance circles; increasing series capacitive reactance moves an impedance point counter-clockwise along these circles. In this case, the circle to be used for finding series  $C$  is the one passing through the center of the chart, as shown by the solid line in Fig. 6.

Increasing shunt inductive susceptance moves impedance points clockwise along constant-conductance circles. These circles are like the constant-resistance circles, but they are on another Smith Chart, this one being just the reverse of the one in Fig. 6. The constant-conductance circles for shunt  $L$  all pass through the leftmost point of the chart rather than the rightmost point. The circles to be used are those passing through  $s_{11}^*$  and  $s_{22}^*$ , as shown by the dashed lines in Fig. 6.

Once these circles have been located, the normalized values of  $L$  and  $C$  needed for the matching networks are calculated from readings taken from the reactance and susceptance scales of the Smith Charts. Each element's reactance or susceptance is the difference between the scale readings at the two end points of a circular arc. Which arc corresponds to which element is indicated in Fig. 6. The final network and the element values, normalized and unnormalized, are shown in Fig. 7.

### Broadband Amplifier Design

Designing a broadband amplifier, that is, one which has nearly constant gain over a prescribed frequency range, is a matter of surrounding a transistor with external elements in order to compensate for the variation of forward gain  $|s_{21}|$  with frequency. This can be done in either of two ways — first, negative feedback, or second, selective mismatching of the input and output circuitry. We will use the second method. When feedback is used, it is usually convenient to convert to y- or z-parameters (for shunt or series feedback respectively) using the conversion equations given in the table, p. 24, and a digital computer.

Equation 24 for the unilateral transducer power gain can be factored into three parts:

$$G_{Tu} = G_o G_1 G_2$$

where

$$G_o = |s_{21}|^2$$

$$G_1 = \frac{1 - |\Gamma_s|^2}{|1 - s_{11}\Gamma_s|^2}$$

$$G_2 = \frac{1 - |\Gamma_L|^2}{|1 - s_{22}\Gamma_L|^2}$$

When a broadband amplifier is designed by selective mismatching, the gain contributions of  $G_1$  and  $G_2$  are varied to compensate for the variations of  $G_o = |s_{21}|^2$  with frequency.

Suppose that the 2N3478 transistor whose s-parameters are given in Fig. 4 is to be used in a broadband amplifier which has a constant gain of 10 dB over a frequency range of 300 MHz to 700 MHz. The amplifier is to be driven from a 50Ω source and is to drive a 50Ω load. According to Fig. 5,

$$\begin{aligned} |s_{21}|^2 &= 13 \text{ dB at } 300 \text{ MHz} \\ &= 10 \text{ dB at } 450 \text{ MHz} \\ &= 6 \text{ dB at } 700 \text{ MHz} . \end{aligned}$$

To realize an amplifier with a constant gain of 10 dB, source and load matching networks must be found which will decrease the gain by 3 dB at 300 MHz, leave the gain the same at 450 MHz, and increase the gain by 4 dB at 700 MHz.

Although in the general case both a source matching network and a load matching network would be designed,  $G_{1\max}$  (i.e.,  $G_1$  for  $\Gamma_s = s_{11}^*$ ) for this transistor is less than 1 dB over the frequencies of interest, which means there is little to be gained by matching the source. Consequently, for this example, only a load-matching network will be designed. Procedures for designing source-matching networks are identical to those used for designing load-matching networks.

The first step in the design is to plot  $s_{22}^*$  over the required frequency range on the Smith Chart, Fig. 8. Next, a set of constant-gain circles is drawn. Each circle is drawn for a single frequency; its center is on a line between the center of the Smith Chart and the point representing  $s_{22}^*$  at that frequency. The distance from the center of the Smith Chart to the center of the constant gain circle is given by (these equations also appear in the table, p. 23):

$$r_2 = \frac{g_2 |s_{22}|}{1 - |s_{22}|^2 (1 - g_2)}$$

where

$$g_2 = \frac{G_2}{G_{2\max}} = G_2 (1 - |s_{22}|^2)$$

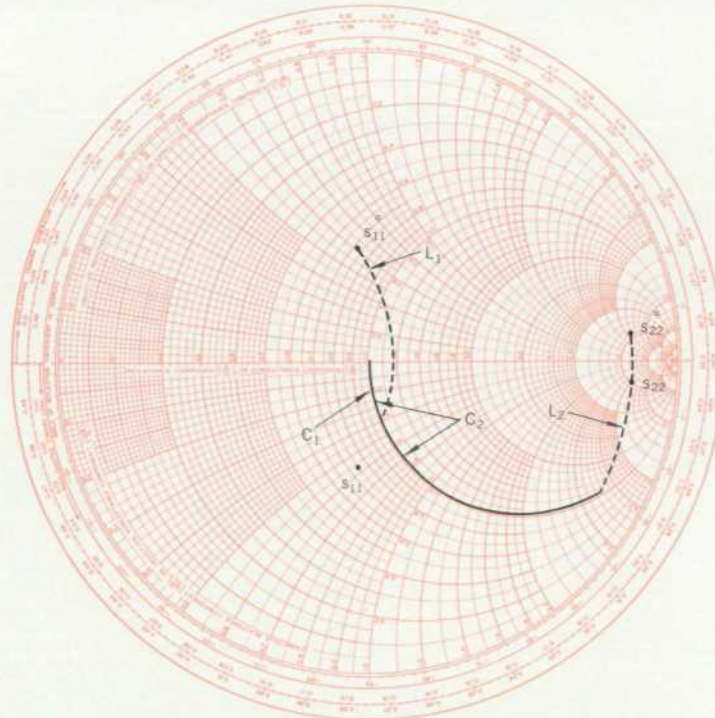


Fig. 6. Smith Chart for 300-MHz amplifier design example.

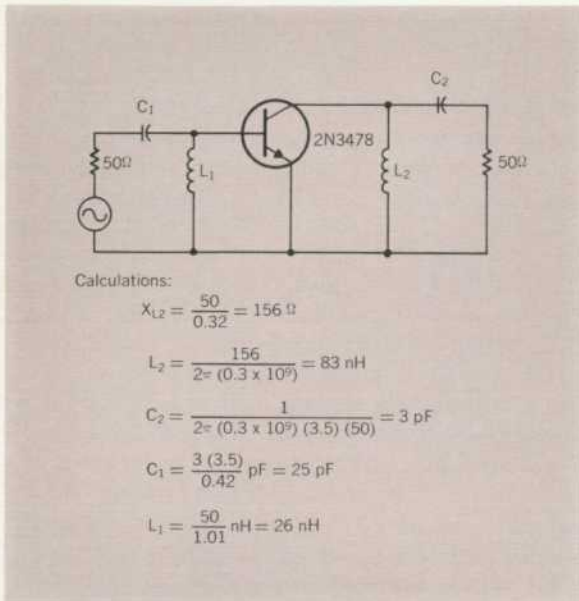


Fig. 7. 300-MHz amplifier with matching networks for maximum power gain.

The radius of the constant-gain circle is

$$\rho_2 = \frac{\sqrt{1 - g_2(1 - |s_{22}|^2)}}{1 - |s_{22}|^2(1 - g_2)}$$

For this example, three circles will be drawn, one for  $G_2 = -3$  dB at 300 MHz, one for  $G_2 = 0$  dB at 450 MHz, and one for  $G_2 = +4$  dB at 700 MHz. Since  $|s_{22}|$  for this transistor is constant at 0.85 over the frequency range [see Fig. 4(b)],  $G_{2 \text{ max}}$  for all three circles is  $(0.278)^{-1}$ , or 5.6 dB. The three constant-gain circles are indicated in Fig. 8.

The required matching network must transform the center of the Smith Chart, representing  $50\Omega$ , to some point on the  $-3$  dB circle at 300 MHz, to some point on the  $0$  dB circle at 450 MHz, and to some point on the  $+4$  dB circle at 700 MHz. There are undoubtedly many networks that will do this. One which is satisfactory is a combination of two inductors, one in shunt and one in series, as shown in Fig. 9.

Shunt and series elements move impedance points on the Smith Chart along constant-conductance and constant-resistance circles, as I explained in the narrow-band design example which preceded this broadband example. The shunt inductance transforms the  $50\Omega$  load along a circle of constant conductance and varying (with frequency) inductive susceptance. The series inductor transforms the combination of the  $50\Omega$  load and the shunt inductance along circles of constant resistance and varying inductive reactance.

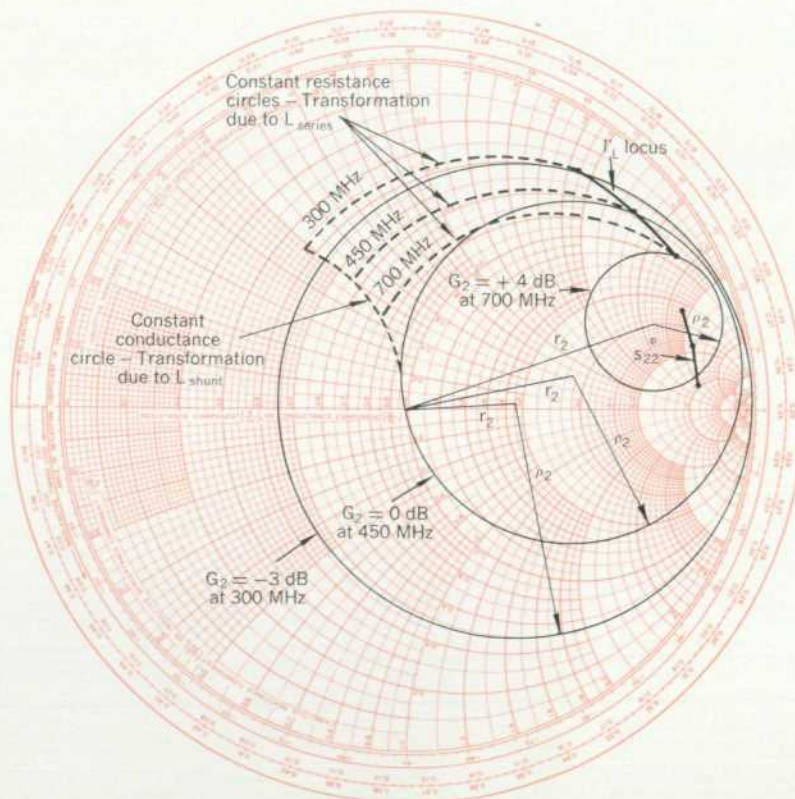


Fig. 8. Smith Chart for broadband amplifier design example.

Optimizing the values of shunt and series L is a cut-and-try process to adjust these elements so that

- the transformed load reflection terminates on the right gain circle at each frequency, and
- the susceptance component decreases with frequency and the reactance component increases with frequency. (This rule applies to inductors; capacitors would behave in the opposite way.)

Once appropriate constant-conductance and constant-resistance circles have been found, the reactances and susceptances of the elements can be read directly from the Smith Chart. Then the element values are calculated, the same as they were for the narrow-band design.

Fig. 10 is a schematic diagram of the completed broadband amplifier, with unnormalized element values.

### Stability Considerations and the Design of Reflection Amplifiers and Oscillators

When the real part of the input impedance of a network is negative, the corresponding input reflection coefficient (equation 17) is greater than one, and the network can be used as the basis for two important types of circuits, reflection amplifiers and oscillators. A reflection amplifier (Fig. 11) can be realized with a circulator—a nonreciprocal three-port device—and a negative-resistance device. The circulator is used to separate the incident (input) wave from the larger wave reflected by the negative-resistance device. Theoretically, if the circulator is perfect and has a positive real characteristic impedance  $Z_0$ , an amplifier with infinite gain can be built by selecting a negative-resistance device whose input impedance has a real part equal to  $-Z_0$  and an imaginary part equal to zero (the imaginary part can be set equal to zero by tuning, if necessary).

Amplifiers, of course, are not supposed to oscillate, whether they are reflection amplifiers or some other kind. There is a convenient criterion based upon scattering parameters for determining whether a device is stable or potentially unstable with given source and load impedances. Referring again to the flow graph of Fig. 3, the ratio of the reflected voltage wave  $b_1$  to the input voltage wave  $b_s$  is

$$\frac{b_1}{b_s} = \frac{s'_{11}}{1 - \Gamma_s s'_{11}}$$

where  $s'_{11}$  is the input reflection coefficient with  $\Gamma_s = 0$  (that is,  $Z_s = Z_0$ ) and an arbitrary load impedance  $Z_L$ , as defined in equation 19.

If at some frequency

$$\Gamma_s s'_{11} = 1 \quad (25)$$

the circuit is unstable and will oscillate at that frequency. On the other hand, if

$$|s'_{11}| < \left| \frac{1}{\Gamma_s} \right|$$

the device is unconditionally stable and will not oscillate, whatever the phase angle of  $\Gamma_s$  might be.

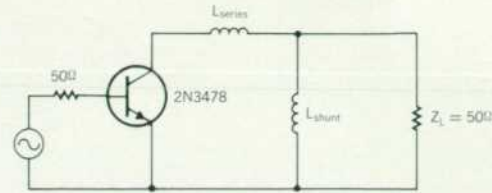
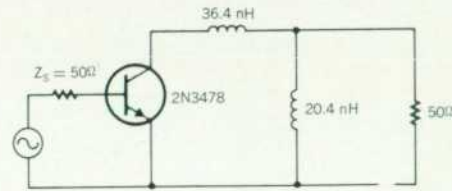


Fig. 9. Combination of shunt and series inductances is suitable matching network for broadband amplifier.



Inductance calculations:

$$\text{From 700 MHz data, } \frac{j\omega L_{\text{series}}}{Z_0} = j(3.64 - 0.44) = j3.2$$

$$L_{\text{series}} = \frac{(3.2)(50)}{2\pi(0.7)} \text{ nH} = 36.4 \text{ nH}$$

$$\text{From 300 MHz data, } \frac{Z_0}{j\omega L_{\text{shunt}}} = -j1.3$$

$$L_{\text{shunt}} = \frac{50}{(1.3)(2\pi)(0.3)} = 20.4 \text{ nH}$$

Fig. 10. Broadband amplifier with constant gain of 10 dB from 300 MHz to 700 MHz.

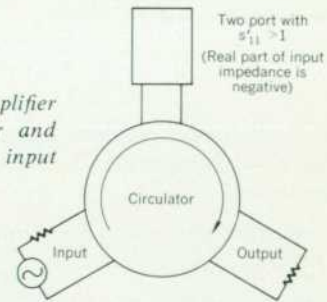


Fig. 11. Reflection amplifier consists of circulator and transistor with negative input resistance.

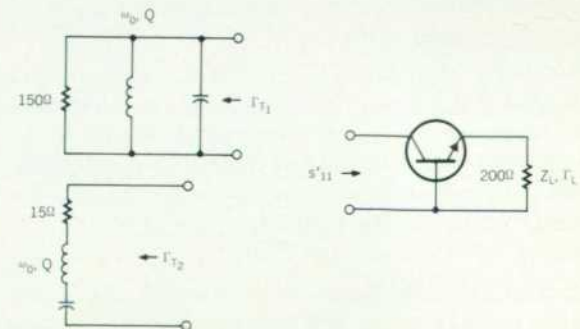


Fig. 12. Transistor oscillator is designed by choosing tank circuit such that  $\Gamma_T s'_{11} = 1$ .

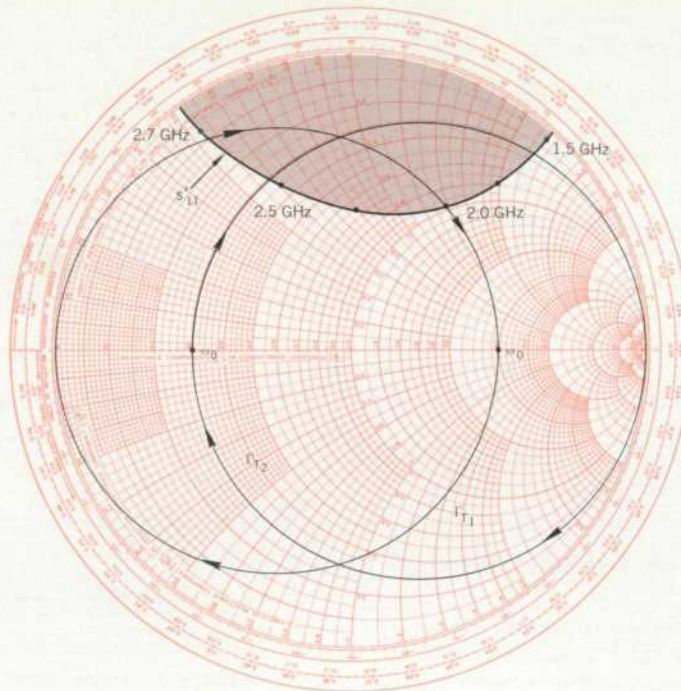


Fig. 13. Smith Chart for transistor oscillator design example.

As an example of how these principles of stability are applied in design problems, consider the transistor oscillator design illustrated in Fig. 12. In this case the input reflection coefficient  $s'_{11}$  is the reflection coefficient looking into the collector circuit, and the 'source' reflection coefficient  $\Gamma_s$  is one of the two tank-circuit reflection coefficients,  $\Gamma_{T1}$  or  $\Gamma_{T2}$ . From equation 19,

$$s'_{11} = s_{11} + \frac{s_{12} s_{21} \Gamma_L}{1 - s_{22} \Gamma_L}$$

To make the transistor oscillate,  $s'_{11}$  and  $\Gamma_s$  must be adjusted so that they satisfy equation 25. There are four steps in the design procedure:

- Measure the four scattering parameters of the transistor as functions of frequency.
- Choose a load reflection coefficient  $\Gamma_L$ , which makes  $s'_{11}$  greater than unity. In general, it may also take an external feedback element which increases  $s_{12} s_{21}$  to make  $s'_{11}$  greater than one.
- Plot  $1/s'_{11}$  on a Smith Chart. (If the new network analyzer is being used to measure the s-parameters of the transistor,  $1/s'_{11}$  can be measured directly by reversing the reference and test channel connections between the reflection test unit and the harmonic frequency converter. The polar display with a Smith Chart overlay will then give the desired plot immediately.)
- Connect either the series or the parallel tank circuit to the collector circuit and tune it so that  $\Gamma_{T1}$  or  $\Gamma_{T2}$  is large enough to satisfy equation 25 (the tank circuit reflection coefficient plays the role of  $\Gamma_s$  in this equation).

Fig. 13 shows a Smith Chart plot of  $1/s'_{11}$  for a high-frequency transistor in the common-base configuration. Load impedance  $Z_L$  is  $200\Omega$ , which means that  $\Gamma_L$ , referred to  $50\Omega$  is 0.6. Reflection coefficients  $\Gamma_{T1}$  and  $\Gamma_{T2}$  are also plotted as functions of the resonant frequencies of the two tank circuits. Oscillations occur when the locus of  $\Gamma_{T1}$  or  $\Gamma_{T2}$  passes through the shaded region. Thus this transistor would oscillate from 1.5 to 2.5 GHz with a series tuned circuit and from 2.0 to 2.7 GHz with a parallel tuned circuit.

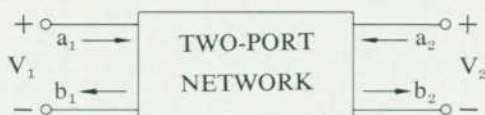
—Richard W. Anderson

#### Additional Reading on S-Parameters

Besides the papers referenced in the footnotes of the article, the following articles and books contain information on s-parameter design procedures and flow graphs.

- F. Weinert, 'Scattering Parameters Speed Design of High-Frequency Transistor Circuits', *Electronics*, Vol. 39, No. 18, Sept. 5, 1966.
- G. Fredricks, 'How to Use S-Parameters for Transistor Circuit Design', *EEE*, Vol. 14, No. 12, Dec., 1966.
- D. C. Youla, 'On Scattering Matrices Normalized to Complex Port Numbers', *Proc. IRE*, Vol. 49, No. 7, July, 1961.
- J. G. Linvill and J. F. Gibbons, 'Transistors and Active Circuits', McGraw-Hill, 1961. (No s-parameters, but good treatment of Smith Chart design methods.)

## Useful Scattering Parameter Relationships



$$b_1 = s_{11}a_1 + s_{12}a_2$$

$$b_2 = s_{21}a_1 + s_{22}a_2$$

Input reflection coefficient with arbitrary  $Z_L$

$$s'_{11} = s_{11} + \frac{s_{12}s_{21}\Gamma_L}{1 - s_{22}\Gamma_L}$$

Output reflection coefficient with arbitrary  $Z_S$

$$s'_{22} = s_{22} + \frac{s_{12}s_{21}\Gamma_S}{1 - s_{11}\Gamma_S}$$

Voltage gain with arbitrary  $Z_L$  and  $Z_S$

$$A_V = \frac{V_2}{V_1} = \frac{s_{21}(1 + \Gamma_L)}{(1 - s_{22}\Gamma_L)(1 + s'_{11})}$$

Power Gain =  $\frac{\text{Power delivered to load}}{\text{Power input to network}}$

$$G = \frac{|s_{21}|^2(1 - |\Gamma_L|^2)}{(1 - |s_{11}|^2) + |\Gamma_L|^2(|s_{22}|^2 - |D|^2) - 2 \operatorname{Re}(\Gamma_L N)}$$

Available Power Gain =  $\frac{\text{Power available from network}}{\text{Power available from source}}$

$$G_A = \frac{|s_{21}|^2(1 - |\Gamma_S|^2)}{(1 - |s_{22}|^2) + |\Gamma_S|^2(|s_{11}|^2 - |D|^2) - 2 \operatorname{Re}(\Gamma_S M)}$$

Transducer Power Gain =  $\frac{\text{Power delivered to load}}{\text{Power available from source}}$

$$G_T = \frac{|s_{21}|^2(1 - |\Gamma_S|^2)(1 - |\Gamma_L|^2)}{|(1 - s_{11}\Gamma_S)(1 - s_{22}\Gamma_L) - s_{12}s_{21}\Gamma_S\Gamma_L|^2}$$

Unilateral Transducer Power Gain ( $s_{12} = 0$ )

$$G_{Tu} = \frac{|s_{21}|^2(1 - |\Gamma_S|^2)(1 - |\Gamma_L|^2)}{|1 - s_{11}\Gamma_S|^2 |1 - s_{22}\Gamma_L|^2}$$

$$= G_0 G_1 G_2$$

$$G_0 = |s_{21}|^2$$

$$G_1 = \frac{1 - |\Gamma_S|^2}{|1 - s_{11}\Gamma_S|^2}$$

$$G_2 = \frac{1 - |\Gamma_L|^2}{|1 - s_{22}\Gamma_L|^2}$$

Maximum Unilateral Transducer Power Gain when  $|s_{11}| < 1$  and  $|s_{22}| < 1$

$$G_u = \frac{|s_{21}|^2}{|(1 - |s_{11}|^2)(1 - |s_{22}|^2)|}$$

$$= G_0 G_{1 \max} G_{2 \max}$$

$$G_{i \max} = \frac{1}{1 - |s_{ii}|^2} \quad i = 1, 2$$

This maximum attained for  $\Gamma_S = s_{11}^*$  and  $\Gamma_L = s_{22}^*$

Constant Gain Circles (Unilateral case:  $s_{12} = 0$ )

—center of constant gain circle is on line between center of Smith Chart and point representing  $s_{11}^*$

—distance of center of circle from center of Smith Chart:

$$r_i = \frac{g_i |s_{ii}|}{1 - |s_{ii}|^2 (1 - g_i)}$$

—radius of circle:

$$\rho_i = \frac{\sqrt{1 - g_i}(1 - |s_{ii}|^2)}{1 - |s_{ii}|^2 (1 - g_i)}$$

where:  $i = 1, 2$

$$\text{and } g_i = \frac{G_i}{G_{i \max}} = G_i (1 - |s_{ii}|^2)$$

Unilateral Figure of Merit

$$u = \frac{|s_{11}s_{22}s_{12}s_{21}|}{|(1 - |s_{11}|^2)(1 - |s_{22}|^2)|}$$

Error Limits on Unilateral Gain Calculation

$$\frac{1}{(1 + u^2)} < \frac{G_T}{G_{Tu}} < \frac{1}{(1 - u^2)}$$

### HEWLETT-PACKARD JOURNAL

TECHNICAL INFORMATION FROM THE  
LABORATORIES OF THE HEWLETT-PACKARD COMPANY

**hp** FEBRUARY 1967 Volume 18 • Number 6

PUBLISHED AT THE CORPORATE OFFICES  
1501 PAGE MILL ROAD, PALO ALTO, CALIFORNIA 94304  
Staff: F. J. BURKHARD, Editor; R. P. DOLAN, L. D. SHERGALIS  
R. A. ERICKSON, Art Director

Conditions for Absolute Stability

No passive source or load will cause network to oscillate if a, b, and c are all satisfied.

- a.  $|s_{11}| < 1, |s_{22}| < 1$
- b.  $\left| \frac{|s_{12}s_{21}| - |M^*|}{|s_{11}|^2 - |D|^2} \right| > 1$
- c.  $\left| \frac{|s_{12}s_{21}| - |N^*|}{|s_{22}|^2 - |D|^2} \right| > 1$

Condition that a two-port network can be simultaneously matched with a positive real source and load:

$K > 1$  or  $C < 1$   
 $C = \text{Linville C factor}$

Linville C Factor

$C = K^{-1}$   

$$K = \frac{1 + |D|^2 - |s_{11}|^2 - |s_{22}|^2}{2 |s_{12}s_{21}|}$$

Source and Load for Simultaneous Match

$$\Gamma_{ms} = M^* \left[ \frac{B_1 \pm \sqrt{B_1^2 - 4|M|^2}}{2|M|^2} \right]$$

$$\Gamma_{mL} = N^* \left[ \frac{B_2 \pm \sqrt{B_2^2 - 4|N|^2}}{2|N|^2} \right]$$

Where  $B_1 = 1 + |s_{11}|^2 - |s_{22}|^2 - |D|^2$   
 $B_2 = 1 + |s_{22}|^2 - |s_{11}|^2 - |D|^2$

Maximum Available Power Gain

If  $K > 1$ ,  

$$G_{A \max} = \left| \frac{s_{21}}{s_{12}} (K \pm \sqrt{K^2 - 1}) \right|$$
  
 $K = C^{-1}$   
 $C = \text{Linville C Factor}$

(Use plus sign when  $B_1$  is positive, minus sign when  $B_1$  is negative. For definition of  $B_1$  see 'Source and Load for Simultaneous Match,' elsewhere in this table.)

$D = s_{11}s_{22} - s_{12}s_{21}$

$M = s_{11} - D s_{22}^*$

$N = s_{22} - D s_{11}^*$

s-parameters in terms of h-, y-, and z-parameters	h-, y-, and z-parameters in terms of s-parameters
$s_{11} = \frac{(z_{11} - 1)(z_{22} + 1) - z_{12}z_{21}}{(z_{11} + 1)(z_{22} + 1) - z_{12}z_{21}}$	$z_{11} = \frac{(1 + s_{11})(1 - s_{22}) + s_{12}s_{21}}{(1 - s_{11})(1 - s_{22}) - s_{12}s_{21}}$
$s_{12} = \frac{2z_{12}}{(z_{11} + 1)(z_{22} + 1) - z_{12}z_{21}}$	$z_{12} = \frac{2s_{12}}{(1 - s_{11})(1 - s_{22}) - s_{12}s_{21}}$
$s_{21} = \frac{2z_{21}}{(z_{11} + 1)(z_{22} + 1) - z_{12}z_{21}}$	$z_{21} = \frac{2s_{21}}{(1 - s_{11})(1 - s_{22}) - s_{12}s_{21}}$
$s_{22} = \frac{(z_{11} + 1)(z_{22} - 1) - z_{12}z_{21}}{(z_{11} + 1)(z_{22} + 1) - z_{12}z_{21}}$	$z_{22} = \frac{(1 + s_{22})(1 - s_{11}) + s_{12}s_{21}}{(1 - s_{11})(1 - s_{22}) - s_{12}s_{21}}$
$s_{11} = \frac{(1 - y_{11})(1 + y_{22}) - y_{12}y_{21}}{(1 + y_{11})(1 + y_{22}) - y_{12}y_{21}}$	$y_{11} = \frac{(1 + s_{22})(1 - s_{11}) + s_{12}s_{21}}{(1 + s_{11})(1 + s_{22}) - s_{12}s_{21}}$
$s_{12} = \frac{-2y_{12}}{(1 + y_{11})(1 + y_{22}) - y_{12}y_{21}}$	$y_{12} = \frac{-2s_{12}}{(1 + s_{11})(1 + s_{22}) - s_{12}s_{21}}$
$s_{21} = \frac{-2y_{21}}{(1 + y_{11})(1 + y_{22}) - y_{12}y_{21}}$	$y_{21} = \frac{-2s_{21}}{(1 + s_{11})(1 + s_{22}) - s_{12}s_{21}}$
$s_{22} = \frac{(1 + y_{11})(1 - y_{22}) - y_{12}y_{21}}{(1 + y_{11})(1 + y_{22}) - y_{12}y_{21}}$	$y_{22} = \frac{(1 + s_{11})(1 - s_{22}) + s_{12}s_{21}}{(1 + s_{22})(1 + s_{11}) - s_{12}s_{21}}$
$s_{11} = \frac{(h_{11} - 1)(h_{22} + 1) - h_{12}h_{21}}{(h_{11} + 1)(h_{22} + 1) - h_{12}h_{21}}$	$h_{11} = \frac{(1 + s_{11})(1 + s_{22}) - s_{12}s_{21}}{(1 - s_{11})(1 + s_{22}) + s_{12}s_{21}}$
$s_{12} = \frac{2h_{12}}{(h_{11} + 1)(h_{22} + 1) - h_{12}h_{21}}$	$h_{12} = \frac{2s_{12}}{(1 - s_{11})(1 + s_{22}) + s_{12}s_{21}}$
$s_{21} = \frac{-2h_{21}}{(h_{11} + 1)(h_{22} + 1) - h_{12}h_{21}}$	$h_{21} = \frac{-2s_{21}}{(1 - s_{11})(1 + s_{22}) + s_{12}s_{21}}$
$s_{22} = \frac{(1 + h_{11})(1 - h_{22}) + h_{12}h_{21}}{(h_{11} + 1)(h_{22} + 1) - h_{12}h_{21}}$	$h_{22} = \frac{(1 - s_{22})(1 - s_{11}) - s_{12}s_{21}}{(1 - s_{11})(1 + s_{22}) + s_{12}s_{21}}$

The h-, y-, and z-parameters listed above are all normalized to  $Z_0$ . If  $h'$ ,  $y'$ , and  $z'$  are the actual parameters, then

$z'_{11} = z_{11}Z_0$	$y'_{11} = \frac{y_{11}}{Z_0}$	$h'_{11} = h_{11}Z_0$
$z'_{12} = z_{12}Z_0$	$y'_{12} = \frac{y_{12}}{Z_0}$	$h'_{12} = h_{12}$
$z'_{21} = z_{21}Z_0$	$y'_{21} = \frac{y_{21}}{Z_0}$	$h'_{21} = h_{21}$
$z'_{22} = z_{22}Z_0$	$y'_{22} = \frac{y_{22}}{Z_0}$	$h'_{22} = \frac{h_{22}}{Z_0}$

Transistor Frequency Parameters

- $f_t$  = frequency at which  $|h_{fe}| = |h_{21}|$  for common-emitter configuration = 1
- $f_{max}$  = frequency at which  $G_{A \max} = 1$